Dielectric properties of Carbon nanotubes doped CuTl-1223 superconductor

by:

Zahir Usman

(33-FBAS/MSPHY/F10)

Supervisor:	Co-Supervisor:
Dr. Muhammad Mumtaz	**Dr. Nawazish Ali Khan**
Assistant Professor	Associate Professor
Department of Physics, FBAS,	Department of Physics,
IIU, Islamabad.	QAU, Islamabad.

Department of Physics

Faculty of Basic and Applied Sciences

International Islamic University, Islamabad.
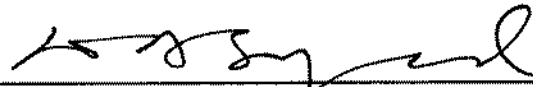
i

Size
-300 dpi
-ock
-small pa.

Carbon
Superconductors
Polarization
Non structure materials.

Dielectric properties of Carbon nanotubes doped CuTl-1223 superconductor
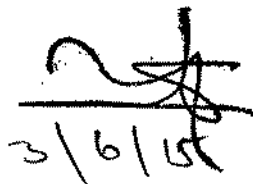
by:

Zahir Usman

(33-FBAS/MSPHY/F-10)

This Thesis submitted to Department of Physics International Islamic University,

Islamabad, for the award of degree of MS Physics.

CHAIRMAN
DEPT. OF PHYSICS
International Islamic University
Islamabad

Chairman Department of Physics

International Islamic University, Islamabad.

Dean Faculty of Basic and Applied Sciences

International Islamic University, Islamabad.

Final Approval

It is certified that the work presented in this thesis entitled **"Dielectric properties of Carbon nanotubes doped CuTl-1223 superconductor"** by **Zahir Usman,** Registration No. 33-FBAS/MSPHY/F-10 fulfills the requirement for the award of degree of MS Physics from Department of Physics, International Islamic University, Islamabad, Pakistan.

Viva Voce Committee

Chairman
(Department of Physics)

Supervisor

Co-Supervisor

External Examiner

Internal Examiner

IN THE NAME OF ALLAH, THE MOST GRACIOUS, THE MOST MERCIFUL

DEDICATED

To

My Dear Parents

&

Beloved Wife

Declaration of Originality

I, **Zahir Usman** (Registration No. 33-FBAS/MSPHY/F-10), student of MS Physics (Session 2010-2012), hereby declare that the work presented in the thesis entitled "**Dielectric properties of Carbon nanotubes doped CuTl-1223 superconductor**" in partial fulfillment of MS degree in Physics from International Islamic University, Islamabad, is my own work and has not been published or submitted as research work or thesis in any form in any other university or institute in Pakistan or aboard.
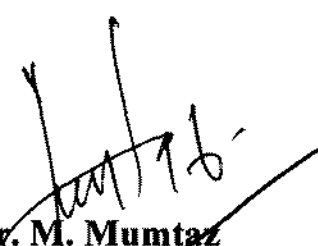
Zahir Usman

(33-FBAS/MSPHY/F-10)

Dated: _____

Forwarding Sheet by Research Supervisor

The thesis entitled **"Dielectric properties of Carbon nanotubes doped CuTl-1223 superconductor"** submitted by **Zahir Usman** (Registration No. 33-FBAS/MSPHY/F-10) in partial fulfillment of MS degree in Physics has been completed under my guidance and supervision. I am satisfied with the quality of his research work and allow him to submit this thesis for further process to graduate with Master of Science degree from Department of Physics, as per International Islamic University, Islamabad rules and regulations.

Dr. M. Mumtaz

Assistant Professor (TTS)

Department of Physics,

International Islamic University,

Islamabad.

Dated: 28/05/2015

Acknowledgement

First and foremost, I would like to say Alhamdulillah, for giving me the strength and health to do this research project until it is done.

I would like to express my sincere gratitude to my project supervisor, **Dr. Muhammad Mumtaz**, whose encouragement, guidance and support from the initial to the final level enabled me to develop an understanding of the subject, who not only guided me, but kept on challenging me to work even harder.

I am also thankful to my project co-supervisor, **Dr. Nawazish Ali Khan** for his guidance at every stage in data collection.

I would like to express my sincere thanks to all the faculty members of Department of Physics IIU Islamabad for their sincere appreciation, comments and suggestions.

I would also like to thank my senior research fellows for extending a helping hand at every juncture of need. They really helped me a lot during whole of my project duration.

I am highly indebted to **Ghulam Hussain**, for guiding me and providing necessary information regarding my project.

Last but not the least, I would like to express my gratitude towards my parents, my family and my wife, without their support my project had not been completed.

Zahir Usman

Table of Contents

List of Figures

Abstract

$(CNTs)_x$/CuTl-1223 nano-superconductor composites were synthesized by solid-state reaction method and investigated by X-ray diffraction (XRD), scanning electron microscopy (SEM) and dc-resistivity. Zero resistivity critical temperature $\{T_c(0)\}$ decreases and normal state resistivity $\{\rho_{300K}(\Omega\text{-m}\}$ increases after the inclusion of CNTs in CuTl-1223 matrix, which indicates the reduction of carriers density and increase of scattering cross-section of mobile carriers after CNTs inclusion. Dielectric properties of $(CNTs)_x$/CuTl-1223 nano-superconductor composites as a function of frequency and temperature were investigated by capacitance (C) and conductance (G) measurements. XRD of samples shows orthorhombic crystal structure following PMMM space group. SEM images show the improved inter-grain weak-links in $(CNTs)_x$/CuTl-1223 nano-superconductor samples. Real part of dielectric constant decreases by increasing wt. % of CNTs, which may likely be due to semiconducting nature of CNTs or due to decrease in polarization after inclusion of CNTs in CuTl-1223 matrix. The negative capacitance (NC) phenomenon has been observed, which is due to positive space charge within the vicinity of electrodes. Imaginary part of dielectric constant increases at lower frequencies with decreasing temperature from 287 K to 92K. Inclusion of CNTs at grain-boundaries reduces polarization and hence affecting dielectric parameters.

Chapter 1

INTRODUCTION

In this chapter we will discuss the basic introduction and a brief history of superconductors, their characteristics, types and different theories in context to superconductors. Dielectrics and mechanisms of polarization are also discussed in this chapter.

1.1 Brief history of Superconductors

A strange phenomenon was observed by Kamerlingh Onnes in 1911 at Leiden laboratory while studying the behavior of mercury at low temperatures. In the vicinity of 4 K, the electrical resistance of mercury disappears completely instead of decreasing gradually [1]. This novel phenomenon was named as superconductivity. A number of experiments were carried out to find the traces of resistance in bulk superconductors but useless. On the basis of modern techniques and equipments it is confirmed that resistivity of the superconductor is zero, at least upto the level of 10^{-24} Ω-m [2].

Later on this phenomenon was observed in other materials like tin, lead, indium, niobium and many others. Different types of alloys and intermetallic compounds in superconducting form are also found. Superconductors may be further classified as low temperature superconductors (LTS) and high temperature superconductors (HTS).
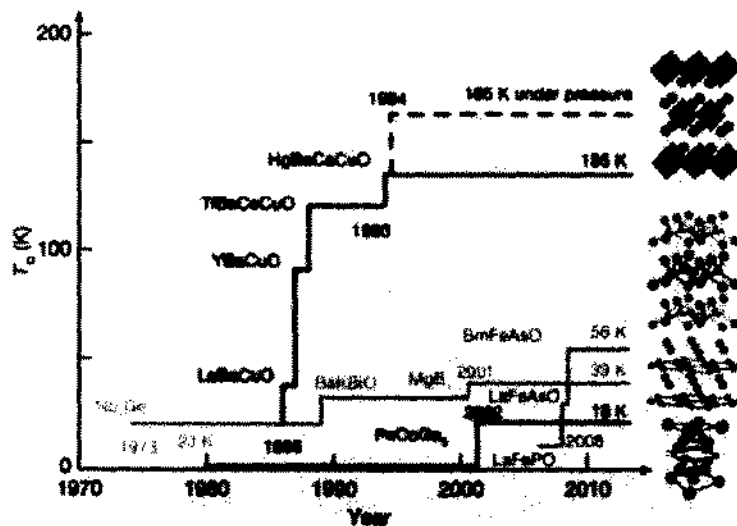
Fig. 1.1: Year wise development in superconductivity

1

Superconductors with transition temperature greater than 77 K ($T_c > 77$ K) are classified as HTS. High temperature layered superconductors like yttrium barium copper oxides(YBCO) and thallium barium calcium copper oxides (TBCCO) are found with critical temperature 92 K and 115 K [3].

Critical temperature 'T_c' is the transition temperature below which normal state changes to superconducting state. This superconducting state can be destroyed by rising temperature by heating the material. This superconductivity can also be affected by magnetic effects. When the superconducting material is placed in weak magnetic field, its superconductivity is destroyed at specific value of magnetic field, called the critical field 'H_c' [4]. This critical field is also called thermodynamic critical field. Temperature dependence of critical field is given by a simple formula,

$$H_c(T) = H_c(0) [1 - (T/T_c)^2] \tag{1.1}$$

1.2 Characteristics of Superconductors

1.2.1 Zero Resistivity

Zero resistivity means infinite conductivity. Below a certain limit of temperature called critical temperature, the resistivity of the material drops to zero. Current flows through it due to the pair of electrons named "cooper pair" [5]. But if the value of current passing through the conductor is greater than the current density J_c, superconductivity disappears.

$$\rho = 0 \text{ for all } T < T_c \tag{1.2}$$

1.2.2 Zero Magnetic Induction

If the material is cooled down below its critical temperature, magnetic induction becomes zero inside it. i.e. magnetic flux is expelled from its interior. There is a certain value of magnetic field called critical field H_c, above which superconductivity disappears [6].
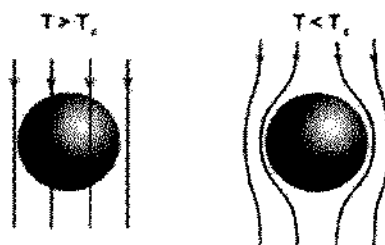
Fig. 1.2: Behaviour of magnetic flux at $T > T_c$ and $T < T_c$

2

1.3   Explanation:

Electric current is set up in the conductors due to flow of charges within the conductors. These moving charges collide with the atoms of the conductor which offer opposition to their flow. The opposition may also arise due to impurities or lattice vibrations (phonon). The measure of opposition offered to these moving charges is known as resistance. This resistance rises by rising the temperature of the conductor. On the other hand if temperature is decreased, resistance decreases. Below a certain temperature called critical temperature resistivity becomes zero. This temperature is also called transition temperature.
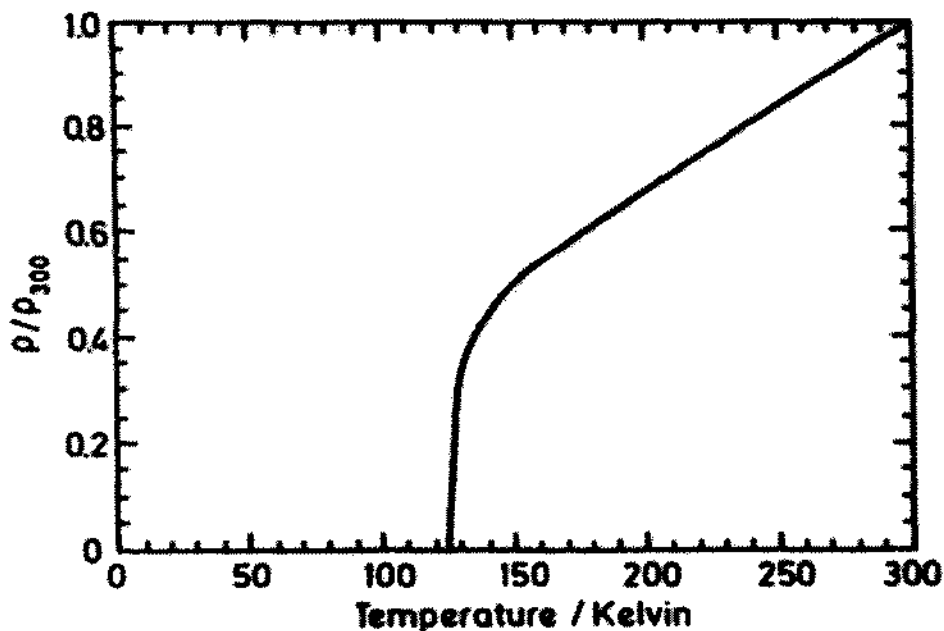
Fig.1.3: Temperature dependence of oxide superconductors.

Electron in normal state repels other electrons according to Coulomb's Law. But if we cool any metal like Aluminum (Al), below its critical temperature T_c, the behavior of electrons changes from their normal state. i.e. gas of repulsive electrons changes into different type of gas in which electrons are present in pairs. A conduction electron of given spin and momentum couples with some other electron of opposite spin and momentum. Lattice vibration called phonons provides attractive force to these couples of electrons called Cooper pairs. This attractive force is responsible for formation of "Cooper Pairs". The electrons in cooper pairs are called 'super electrons'.

3

In normal conductors, impurities are cause of scattering of conduction electrons which results in resistivity of the conductors. While in case of superconductors, the behavior of electrons is quite different. It cannot be done by affecting the ensembles electrons of cooper pairs that take part in superconducting state. As a result, super current establish which keeps on flowing without any dissipation. The cooper pairs make single coherent motion [7]. Also there is no scattering for individual repulsive pair of electrons, means there is no resistivity.
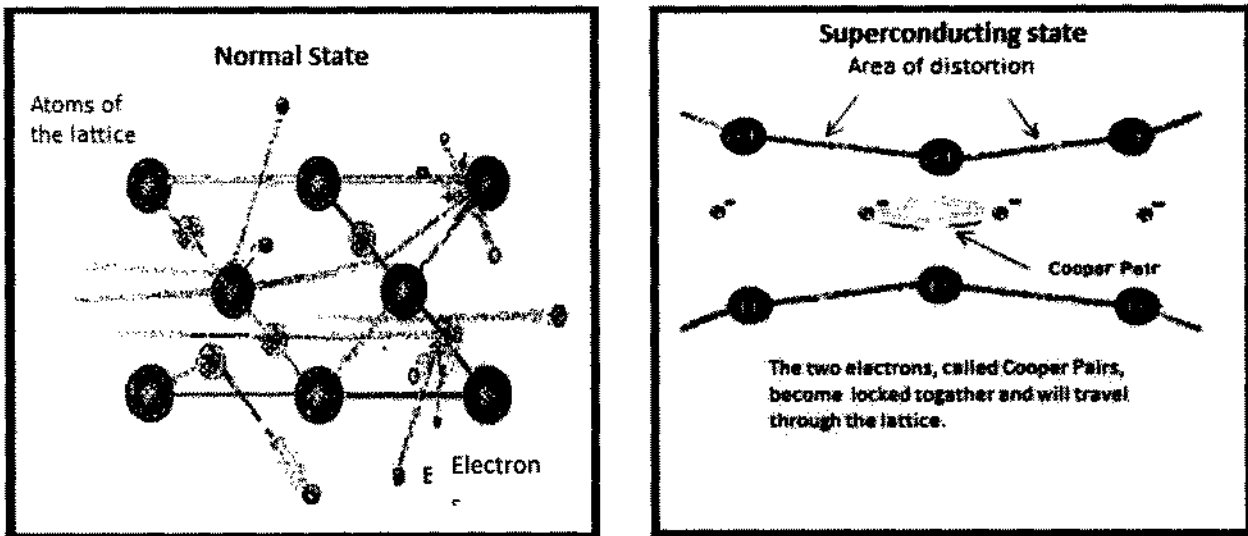
Fig. 1.4: Behavior of electrons in normal state and superconducting state

Fig. 1.4 illustrates the motion of electrons through the lattice. When electron passes through the positive ion cores of the lattice, ion cores deform due to attraction of the electron. This vibration of lattice is named as phonon. Before retreating of this vibration another electron approaches the trough formed by positive ion cores. The phonons exert force on electrons to overcome the repulsive force of electrons. As a result these two electrons called cooper pairs become locked together and travel through the lattice [8].

1.4 Experimental facts of Superconductors

1.4.1 Josephson Effect:

In 1962, evidence of quantum nature of superconducting phenomenon was given by weak superconductivity or Josephson's Effect. Josephson's effect is a situation in which superconductors are attached by tunnel junction.

This effect is divided into two categories,

i. Stationary Josephson effect

ii. Nonstationary Josephson effect

1.4.1.1 Stationary Josephson Effect

Let us first consider the dc effect in which current is applied through the tunnel junction. If amount of current is very small then it will pass through the junction without any resistance [9]. It is because of coherent behavior of the electrons in superconducting state. Superconducting electrons of these superconductors merge into a quantum body.

1.4.1.2 Nonstationary Josephson Effect

This effect is more astonishing than that of dc effect. Keep on increasing the amount of direct current through the weak link till a finite voltage appears across the link. Then along with dc component 'V', voltage also has ac component 'ω' (angular frequency). Relation between 'V' and 'ω' is given by

$$\hbar\omega = 2eV \tag{1.3}$$

1.4.2 The Meissner-Ochsenfeld Effect

A material to be a superconductor must fulfill two characteristics. One is to show zero resistance and second to repel weak magnetic field which is in manifestation of Meissner-Ochsenfeld effect [10].

Consider a conductor in its normal state. If we cool down that conductor below its critical temperature, it changes into superconductor. Initially no magnetic field is applied across the conductor. Then apply magnetic field across it. As per general observation, no field passes through the specimen as shown in Fig 1.5. In fact when applied magnetic field passes through the

specimen, due to change in its flux, current is induced in it. That current also induces a magnetic field which is opposite to that of applied field in accordance with Lenz's Law. Therefore interior of the specimen is field free region. This phenomenon cannot be extracted from law of zero resistivity.

This phenomenon can also be explained by using Maxwell's equation. That is given by

$$\nabla \times E = -\oiint \frac{\partial B}{\delta t} \tag{1.4}$$

$E = 0$ for an ideal conductor. Above equation results

$$\frac{\partial B}{\delta t} = 0 \tag{1.5}$$

at all points inside the superconductor.
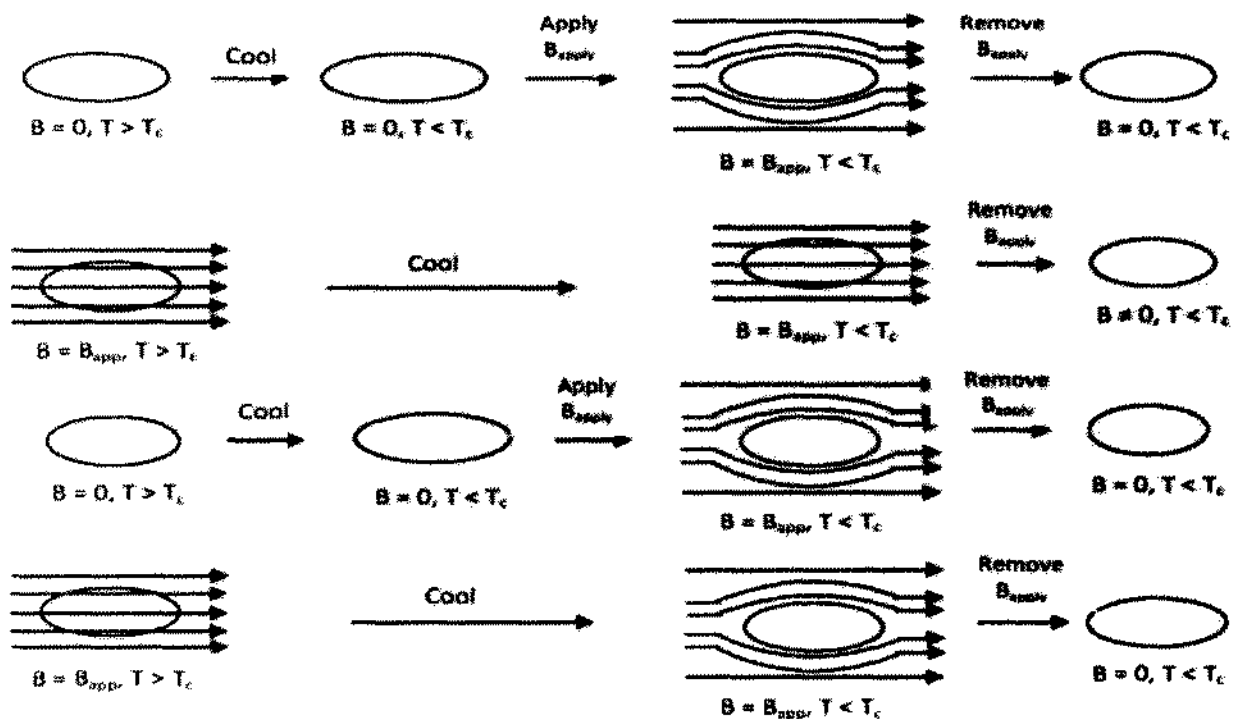
Fig. 1.5: The Meissner-Ochsenfeld Effect

6

Meissner-Ochsenfeld effect is characteristic of thermal equilibrium whereas resistivity is non-equilibrium transport effect. Final state of specimen is independent of the history of specimen. Superconductors may also be defined as a system which exhibit Meissner-Ochsenfeld effect.

1.5   BCS Theory

In 1957, J.Bardeen, L.N. Cooper and J.S.Schrieffer presented a theory named BCS theory. The phenomenon like zero resistivity, Meissner effects etc. were successfully explained on the basis of BCS theory. Two main features of BCS theory are

   i.   Formation of electron pairs (Cooper pair)

   ii.   Propagation without resistance

These pairs move throughout the lattice in resonance with phonons and hence offer zero resistance. BCS theory describes this interaction as electron-phonon interaction [11].
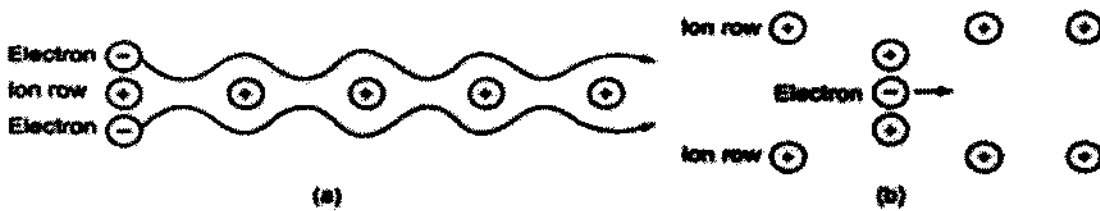
Fig. 1.6: Movement of electrons in (a) one dimensional lattice and (b) between two rows   of a two dimensional lattice.

In case of superconductors, zero resistance can be explained on the basis of BCS theory. The electrons propagate through the ion core. Coulomb's attraction between electron and ion core distort the lattice. As a result phonons are produced.

1.5.1   Prediction of BCS Theory

Predictions of BCS theory are given as under

   i.   Variation of critical field with temperature and isotope effect

   ii.   Existence of energy gap

   iii. Quantization of magnetic flux

   iv. Presence of coherence length

1.5.1.1 Critical field and variation with temperature

This theory could successfully predict the phenomenon of isotope effect and variation of critical field with temperature. BCS theory also predicts the existence of energy gap between the ground and excited states. This gap represents the energy requisite to break the cooper pair. Hence the superconductors with large energy gap are more stable.

1.5.1.2 Isotope Effect

After the discovery of superconducting state, large numbers of theories were proposed but none of them successfully explained the superconducting state of electrons. In 1950, Frohlich proposed that transition temperature of superconductors varies with mass of the isotopes. The phenomenon of increase of transition temperature with increasing atomic mass is called isotope effect. Equation is given by

$$M^{\alpha}T_c = \text{Constant} \tag{1.6}$$

M = Mass of superconducting isotope

α = Varies from material to material, α is about 0.5

This effect indicates that electron phonon interaction is of great importance in superconducting state [12]. This is in contrast with classical model of conduction in which zero interaction between the electron and phonon is effect of zero resistance.

1.5.1.3 Energy Gap

The difference of the energy between the ground state and the superconducting state is called the energy gap. The levels for the electrons in normal state are above the Fermi surface whereas the levels for superconducting electrons are below the Fermi surface. This energy gap is the function of temperature. Energy gap in case of insulators and superconductors is constant.

At absolute temperature i.e at 0 K, this energy gap is maximum. Energy gap at 0 K is given by the relation

$$E_g(0) = 3.54 \, KT_c \tag{1.7}$$

In other words one can say that the pairing of electrons is complete at 0K. But when temperature becomes equal to the critical temperature, pairing of electrons disappear and

therefore energy gap becomes zero and superconducting phenomenon vanish [13]. In range of T = 0 K and T = T_c, there are many ground states and excited states for the superconducting electrons. In such states electron pairs are considered to be in condensed state with complete phase coherence. This phase coherence is below the critical temperature. As critical temperature is attained, phase coherence vanishes and pairs broke up resulting in transition of state i.e. Superconducting material is converted into normal conductor.

1.5.1.4 Quantization of Magnetic Flux

Another prediction of BCS theory is the quantization of magnetic flux in superconductors. To understand this phenomenon consider a bulk superconductor with a hole in it in its normal state i.e $T > T_c$ [14]. Then by applying field H_0 in the direction of axis of cylinder, we decrease the temperature of specimen below its critical temperature, after which specimen changes its state from normal to superconducting. After this, magnetic flux is pushed out from the interior of the superconductor. But some of the flux remains there in the hole. This flux is due to the super current which is induced at the inner surface of hole. This frozen magnetic flux can be found out by following method [1].

Inside the superconductor, consider a contour that encloses the hole such that separation between contour and inner surface of hole is in limit of λ.

$$\frac{\phi_o}{2\pi} \oint_c \nabla \theta \cdot dl = \oint_c A \cdot dl \tag{1.8}$$

As flux is given as

$$\oint_c A \cdot dl = \phi \tag{1.9}$$

Then equation 1.8 becomes

$$\phi = \frac{\phi_o}{2\pi} \oint_c \nabla \theta \cdot dl \tag{1.10}$$

Above is the total flux through the contour. And θ is multi valued function. It changes with change of complete round the contour. It means that magnetic flux should be an integral multiple of 2π i.e. $2\pi n$. Where n=0,1,2,3,.....

9

It means

$$\oint_c \nabla \theta \cdot dl = 2\pi n \tag{1.11}$$

This implies that $\quad\quad\quad\quad \phi = n\phi_0 \tag{1.12}$

Where $\quad\quad\quad\quad\quad \phi_0 = hc/2e \tag{1.13}$

From equation 1.12, it is clear that magnetic flux is quantized because it is integral multiple of threshold value of magnetic flux i.e. ϕ_0. Its numerical value is 2.07×10^{-7} G-cm^2

Magnetic flux quantization was experimentally discovered in 1961 approximately at the same time in USA by B. Deaver and W. Fairbank and in Germany by R. Doll and M. Nabauer. Quantization of magnetic flux was predicted by F. London. He believed that flux quantum must be hc/e. And it is twice as large as ϕ_0.

Experiments confirmed the above mentioned equation 1.13 for ϕ_0. It is clear that the experiments that detected the magnetic flux quantization also confirmed that super current is due to the pair of electrons.

1.5.1.5 Coherence Length

Coherence length is the characteristic property of superconductor. Electron density in superconductor cannot be changed quickly, in fact there is a specific length over which this change can be made. Beyond this, superconducting state disappears. This length is known as coherence length. It depends on Fermi velocity, energy gap of the superconducting material and mean free path of charge carrier [15].

For example, transition of the material from superconducting state to the normal state will have a transition layer of certain thickness which relates to coherence length.

Coherence length is given by

$$\xi_o = \frac{\hbar v_F}{2E_g} \tag{1.14}$$

Where v_f is the Fermi energy and E_g is the energy gap of superconductor.

1.6   Penetration Depth of a Magnetic Field in a Superconductor

Penetration depth is defined as the depth over which strength of field falls exponentially by 'e' times of its original value. Fig 1.7 shows the boundary inside the superconductor with area on its left side and field on right side in the figures is shown by arrow. There are black dots in circle that show the direction of current flowing outside the surface.

Superconducting current flows along the boundary, screens the field to enter into the material.
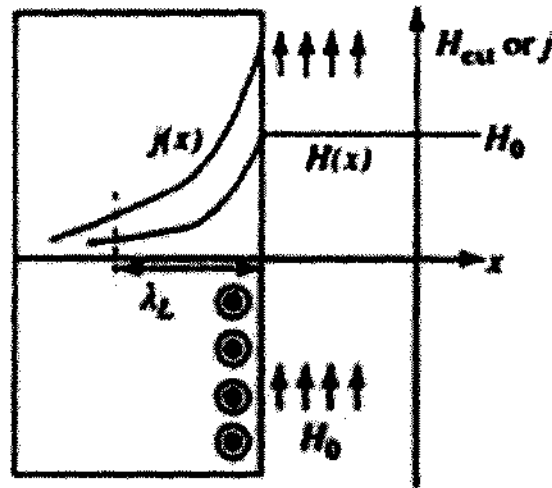
Fig. 1.7:   Penetration depth inside superconducting material from the surface.
Circles represent the surface current.

Superconducting current flows near the surface of the material. If this surface is narrowed, the density of current rises and ultimately material is destroyed. Now if this supercurrent is distributed all over the surface, the field enters upto the same depth inside the superconducting material. The strength of external magnetic field and current density entirely depends on the depth inside the material from the surface. As we proceed along with this depth inside the material, both magnetic field strength and current density decrease gradually.

This penetration depth is also called London Penetration depth [16] and is denoted by λ_L. It depends on the nature of the material and varies from material to material. Penetration depth for different superconducting materials is given in table 1.1.

11

Table 1.1: Penetration depth for different superconducting materials at 0 K

Superconductor	λ_L
Tin	510
Aluminium	500
Lead	390
Mercury	450
Niobium	470
Thallium	920
Indium	640

1.7 Dielectrics

Dielectrics are insulator materials with no free electrons [17]. All the electrons in atoms of insulators are bound and valence band of atoms are completely filled, whereas conduction band is empty. There is also a large energy gap between valence band and conduction band. No electron can jump to overcome this gap. Therefore, a large amount of energy required to excite these electrons from valence band and conduction band. So, virtually, no electron can move to take part in conduction. These dielectric materials can only describe the phenomenon of polarization. These dielectrics can also be characterized by using different parameters to explain their polarization.

1.8 Polarization

Polarization is the microscopic behavior of the dielectric materials. Whenever a material undergoes external applied dc electric field, behavior of the materials entirely depend upon chemical bonding. In case of dielectric material when it is subjected to applied dc electric field, positive nucleus moves slightly in the direction of field and negatively charged electrons move in direction opposite to that of field. As a result, these are separated by small microscopic displacement. And atom no more remains electrically neutral as it becomes electric dipole with dipole moment $p = (Ze) r$ [18]. Also this dipole moment is also directly proportional to E.

$$p = \alpha E \qquad (1.15)$$

12

Unpolarized

Polarized by an applied electric field
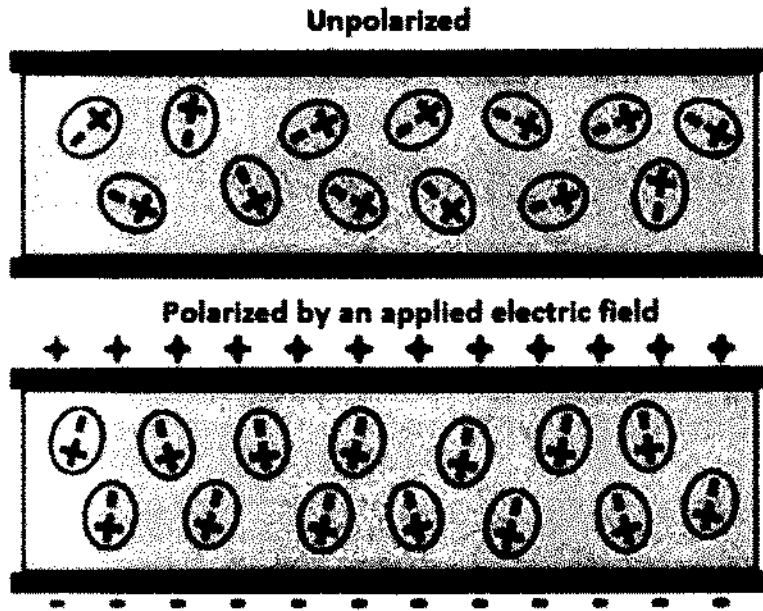
Fig 1.8: Polarization in dielectrics.

1.9 Dielectric Susceptibility

When a dielectric material is placed between the plates of the capacitor or it is subjected to dc electric field, it becomes electrically polarized. Electric susceptibility determines the rate of polarization i.e. how fast the material becomes polarized. Polarization of the material is proportional to applied electric field [19].

$$P = \varepsilon_0 \chi E \tag{1.16}$$

As electric flux density is given by

$$D = \varepsilon E = \varepsilon_0 \varepsilon_r E \tag{1.17}$$

Relation between electric flux density and polarization is

$$P = D - \varepsilon_0 E \tag{1.18}$$

$$P = \varepsilon_0 \varepsilon_r E - \varepsilon_0 E \tag{1.19}$$

$$P = (\varepsilon_r - 1)\varepsilon_0 E \tag{1.20}$$

$$P = \varepsilon_0 \chi E \tag{1.21}$$

Where electric susceptibility 'χ' is given by

$$\chi = \varepsilon_r - 1 \tag{1.22}$$

13

1.10 Mechanisms of Dielectric Polarization

Local applied electric field polarizes the atoms or molecules of dielectrics. Atom is neutral species but only in the absence of field. Once it comes under influence of field, its neutrality vanishes. Positive and negative charges get perturbed by following dielectric mechanisms [20].

- Electronic polarization
- Ionic polarization
- Dipolar or orientation polarization

1.10.1 Electronic Polarization

This type of polarization occurs when an individual neutral atom comes under the influence of electric field. As a result of this, negatively charged electron cloud and positive nucleus are displaced by some distance as shown in Fig. 1.9 [21]. Electronic polarization is induced polarization as it is because of induced dipole moment.
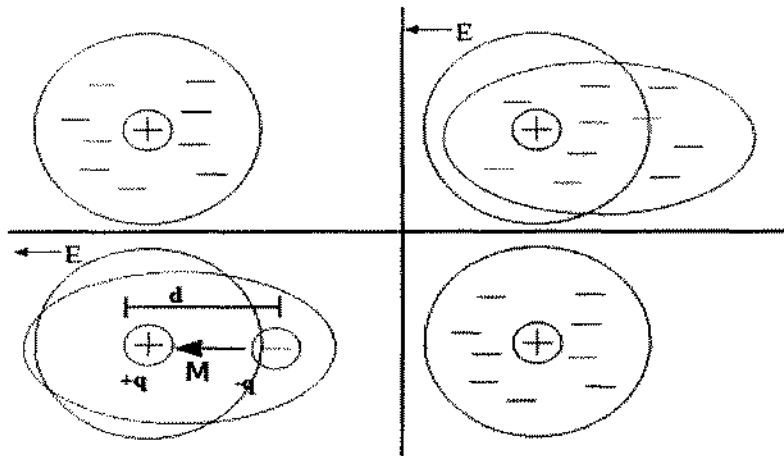
Fig 1.9 : Electronic polarization.

1.10.2 Ionic Polarization

In this type of polarization, those materials are included which have ionic character. Such materials have built in dipole moments but these are oriented in such a way that they exactly cancel each other. When these are subjected to external field, net dipole moment are induced which results in ionic polarization [22].

14
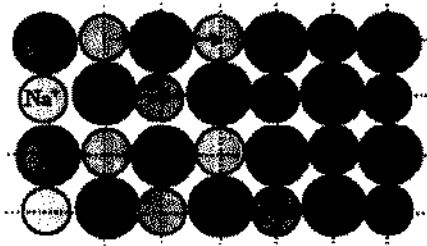
Fig 1.10: Ionic dielectric with zero
electric field.
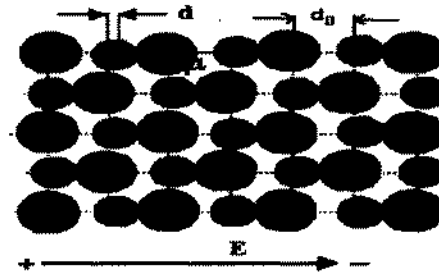
Fig 1.11: Ionic dielectric with applied
electric field.

1.10.3 Dipolar or Orientational Polarization

Some dielectric materials have permanent electric dipole moments as the centers of positive and negative charges do not overlap. Such dielectric materials are called polar dielectrics. In presence of external field electric dipoles of these polar dielectric materials orient themselves in the direction of field as shown in Fig. 1.12. This type of polarization is called dipolar or orientational polarization [23].
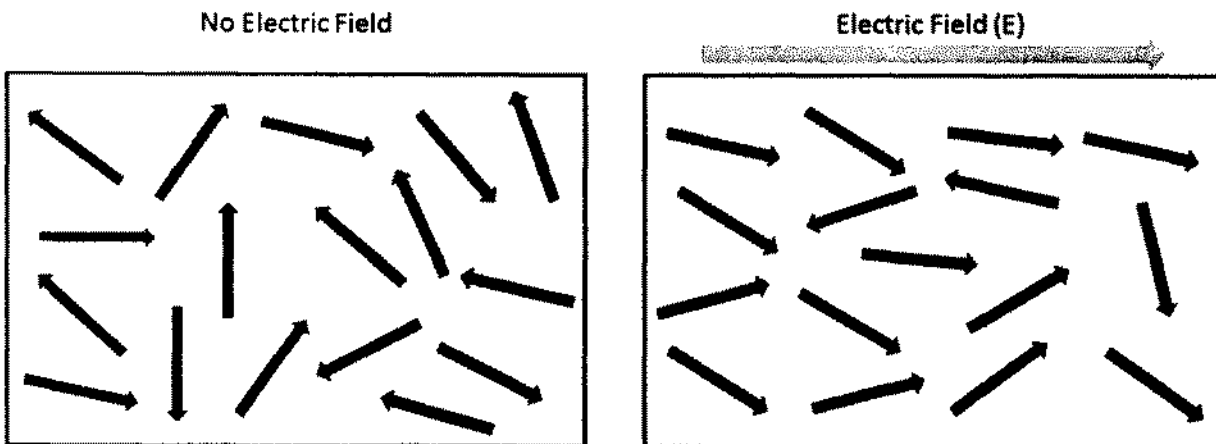
Fig1.12: Dipolar or orientation polarization.

15

1.11 Temperature dependence of Dielectric Constant

Among all the polarizations discussed earlier, only dipolar polarization is the one which is affected by temperature changes. It means only polar dielectrics are effected by temperature. Orientation polarization for liquids and polyatomic gasses relates inversely with temperature and is given by relation

$$P_o = \frac{np^2 E}{3K_B T} \tag{1.23}$$

But in some other polar materials like polymers, increase in temperature causes an increase in dielectric constant as shown in Fig 1.13. This is because of the fact that by increase in temperature, thermal energy increases and dipoles become fewer inhabitants. They only move to get oriented according to field, contributing to polarization P_o.
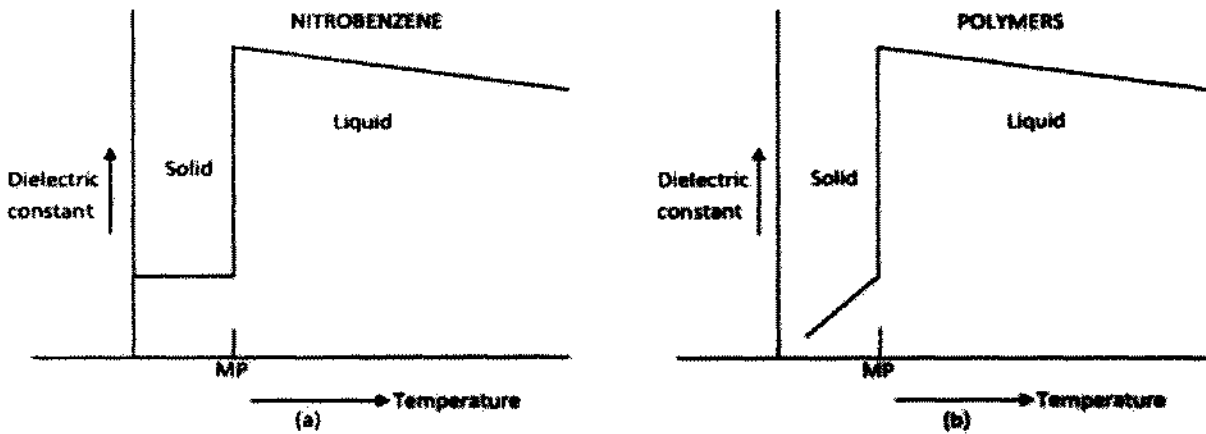
Fig. 1.13: Dependence of dielectric constant on temperature.

1.12 Frequency dependence of Dielectric Constant

When dielectric material undergoes an applied electric field, its frequency affects dielectric constant. Electronic polarization can take place easily and rapidly at high frequencies and energy losses are low [24]. But in case of ionic and dipolar polarization, where alignments of ions and dipoles are involved, response to high frequency is poor. The process of alignment of these ions and dipoles is slow because of inertia. Therefore energy losses are high whereas at low frequencies, these energy losses are low.

16
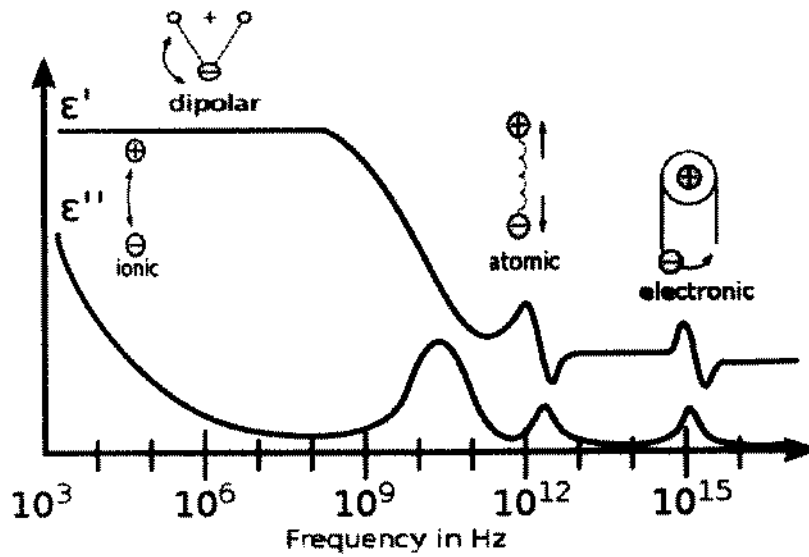
Fig. 1.14: Dependence of dielectric constant on frequency.

1.13 Dielectric Loss

No charge can flow in dielectric practically, it can only displace from its position by polarization. In case of capacitor, current leads the voltage by an angle of 90°. If it is so, there will be no power losses as dielectric will not absorb energy. But practically materials have some losses. Phase angle is not exactly 90°. As compared to ideal dielectric, it lags behind the original angle. This difference of angle is called lag angle and is given by δ. Quantitative measurement of of this angle is tan δ also called *loss-tangent* [25].

$$tan\ \delta\ =\ \frac{\varepsilon_r^{//}}{\varepsilon_r^{/}}$$
(1.24)

Where

$\varepsilon_r^{/}$ = Real part of the dielectric

$\varepsilon_r^{//}$ = Imaginary part of dielectric

17

1.14   Nanoscience and Nanotechnology

Study of very strange behavior of particles of size less than 100 nm is of keen interest in scientific community now a days. Nanoscience is actually the study of particles whose dimensions (at least one) are confined to 100 nm.

1.15   What is Nanometer?

It is the unit to measure the length just like that of meter(SI unit of length). But it is much smaller than that of meter. Nanometer is 1000 million times smaller than meter. Therefore it is impossible to observe such a small length without using specially designed instruments e.g. AFM. A comparison of size of different objects is given below:
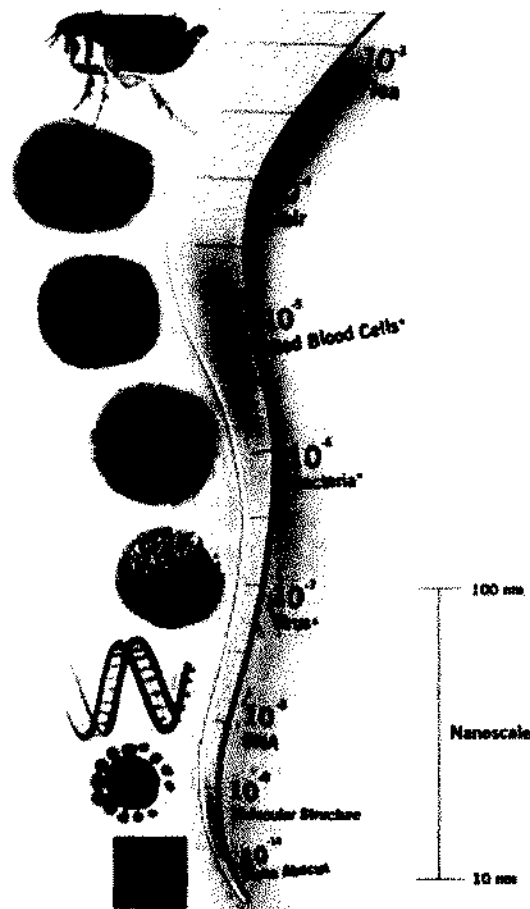
Fig. 1.15: Size of different objects

18

1.16 Nanoscience

Nanoscience is that area of science where size plays very basic and critical role (range: 1nm to 100 nm). If size of the material is reduced upto 100 nm or below then its physical and chemical properties change drastically.

To understand the concept, consider gold particles at bulk level. Now if we cut it into smaller pieces there will be no change in its color upto certain size. But there will be a dramatic change in its color within nanoscale i.e. below 100 nm. Variation of size shape and color in gold nano particles is given below in Fig 1.16.
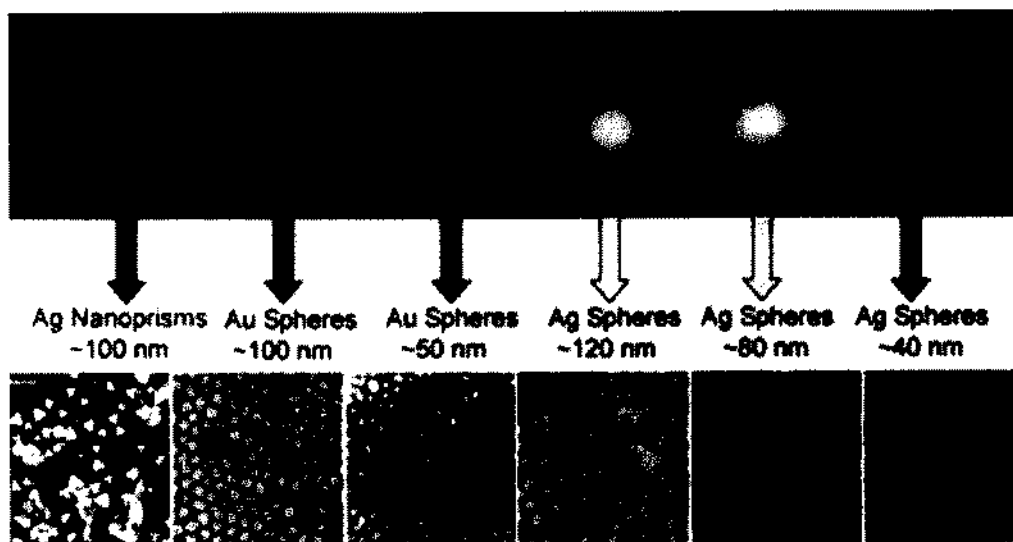
Fig. 1.16: Size, color and shape of Gold nano particles

1.17 Nanotechnology

Nanotechnology is the implementation of nanoscience or it may be called Engineering at nanoscale [26]. As materials at nanoscale exhibit strange and high potential chemical and physical properties which are being used in formation of new useful devices or objects. Nanotechnology is the multi disciplinary area involving physics, chemistry and engineering etc. With the help of all these fields, systems and smallest components are formed at molecular levels which are characterized by large surface area having smaller volume. And quantum mechanical laws define their behavior.

19

1.17.1 Why Nanotechnology?

Materials at nanoscale are very small, then how can they be such important? The question is of great importance. It depends on the use of these nanomaterials. Sometimes these materials are added to some other materials in such a proportion that they entirely change the characteristics of that material. It means nanocomposite materials are formed in accordance with their applications. Scientists and engineers also use materials like nanopowder and nonocrystals to make advanced and more reliable machines and devices. Advancement in the field of nanotechnology may bring revolution in medical and industrial sector in near future [27].
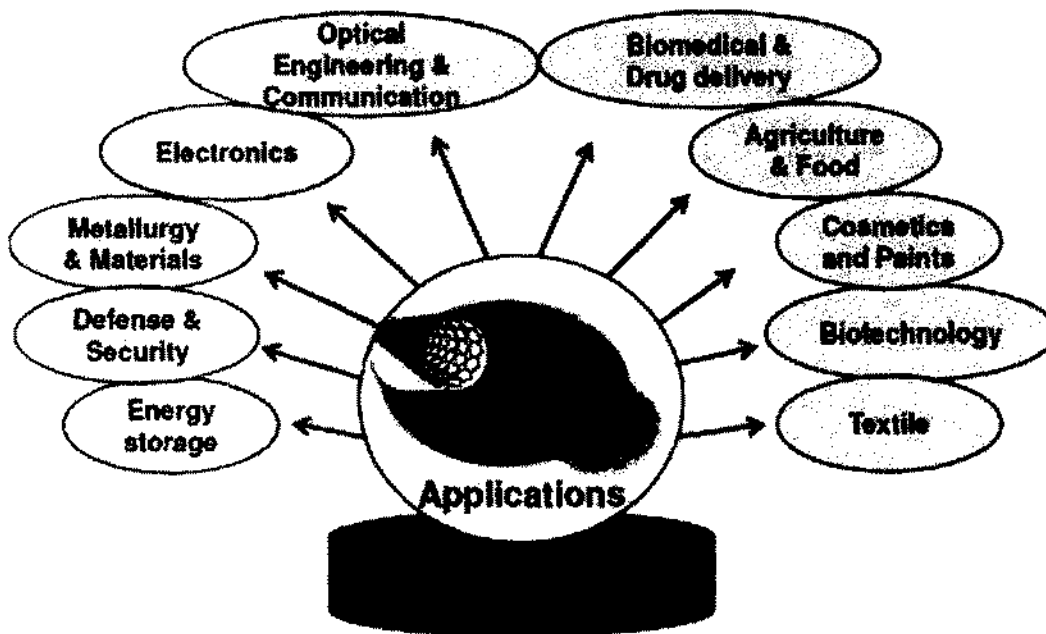
Fig. 1.17: Use of Nanotechnology

1.18 History of Nanotechnology:

In 1959, Couple of questions were asked by **Richard Feynman** (Theoretical Physicist) which lead the scientific lobby to birth of nanotechnology.

- "Is there no way to make an electron microscope more powerful?"
- "Why cannot we write entire 24 volumes of encyclopedia on the head of a pin?"

R. Feynman never used the term nanotechnology.

He said as cells are capable of manufacturing processes then why can't a human being manufacture materials or devices at the same level? He said why can't we manufacture at cellular level or better at atomic level? [27]

It was Norio Taniguchi, Professor of Tokyo Science University who first time used the term 'Nanotechnology'. He was anxious to make the materials of nanoscale tolerance. At nanoscale, the potency of the materials enhances and gravity does not make a much difference. Professor Norio further added that by use of nanotechnology, ultra fine and ultra precise devices can be formed.

But Feynman was well aware of some problems that may rise with reduction of size. The materials may stick together because of attractive forces between the particles of material. A great problem was of large surface area. We can say that laws of chemistry, physics, and quantum mechanics may come into question.

1.19   Techniques of making Nanostructures

There are two main approaches for making nano size structures.
- Top –down Approach.
- Bottom-up approach

1.19.1 Top-down Approach

This method is used to make nanostructure by reducing the size of the material. Lithography is very important in this technique [28]. In lithography first the material is coated with photoresist. Then it is exposed to light. Due to this exposure photochemical reaction takes place which break down the polymer chain. Then after dipping this material in developing solution, exposed areas are detached.
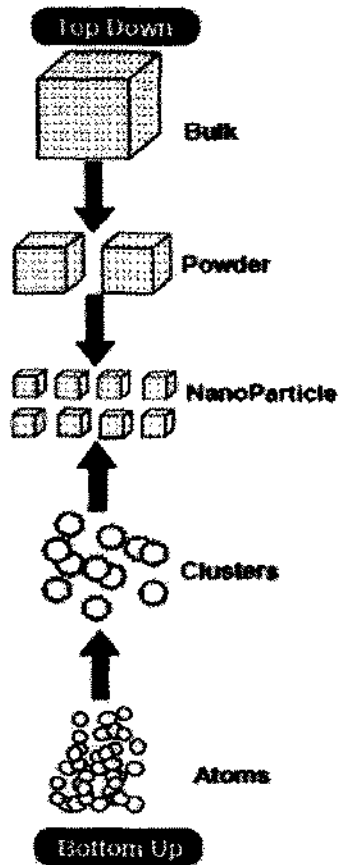
Fig. 1.18: Approaches adopted for nanomaterials

1.19.2 Bottom-up Approach

This approach is also very important in synthesis of nanomaterial. In this technique, nanomaterial is formed by arranging the atoms and molecules by use of different methods. Bottom Up approach includes the methods of vapor deposition, solution method, chemical synthesis, self assembly and positional assembly [29].

Nanostructures can be synthesized by the use of above mentioned techniques. But for their study, different powerful tools are required. With invention of scanning probe microscopes, it became possible for scientists to observe and measure the nanostructures. Atomic force Microscope(AFM) and Scanning Tunneling Microscope (STM) are two powerful tools to observe nanostructures. All other such tools are also based on STM.
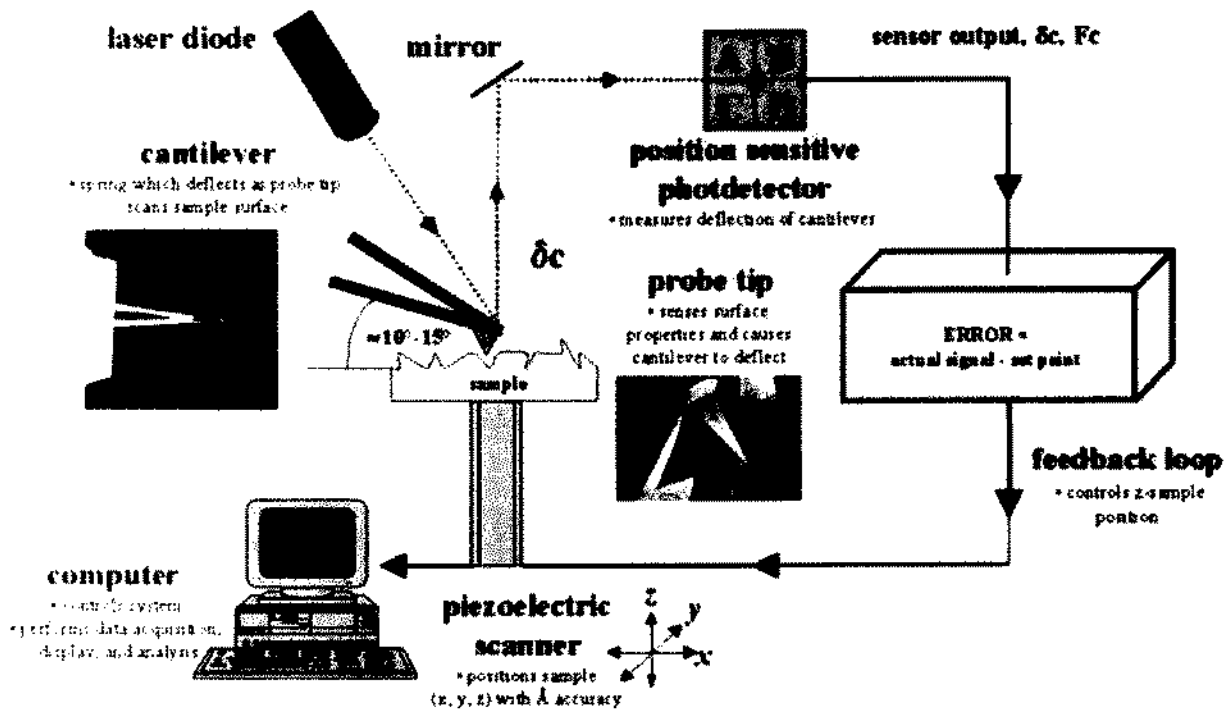
Fig. 1.19: Schematic diagram for Atomic Force Microscopy

Chapter 2

LITERATURE REVIEW

This chapter contains detailed literature review of the superconductors doped with nanoparticles. The critical temperature in case of thallium based superconductor is very high as compared to all the superconducting oxides which have been discovered till date. Among all the high temperature superconductors, $Tl_2Ba_2Ca_{n-1}Cu_nO_x$ is of great importance [30,31]. $Tl_2Ba_2Ca_2Cu_3O_x$ of this system has a critical temperature about 125 K. The value of critical temperature for n=1,(Tl-2201) is 90 K and for n = 2 (Tl-2212) is 110 K.

Cavdar *et al.* [32] prepared a ceramic sample of layered cuprate of $Tl_2Ba_2Ca_1Cu_2O_x$ and $Tl_2Ba_2Ca_2Cu_3O_x$ and investigated the sample by measuring different parameters like dielectric constant, dielectric loss and conductivity. All these parameters were measured as a function of frequency and temperature. During the investigation, variation in frequency was 100 Hz to 1o MHz and for temperature it was 80 – 300 K. They observed negative capacitance effect which is very important in electronics. In contrast to many high temperature superconductors, the dielectric properties of Tl-Ba-Ca-Cu-O (2223+2212) compounds have not been reported yet. They, first time reported the dielectric properties of Tl-Ba-Ca-Cu-O (2223+2212) at the range of frequency 100 h to 10 MHz at temperature range of 80 K to 300 K. X-Rays diffraction pattern showed that material was the mixture of Tl-2212 and Tl-2223. It was confirmed by studying the peak positions and intensities. The dimensions of unit cell for Tl-2212 were a=b=3.845 A and c=29.32A. Unit cell parameters for Tl- 2223 were a = b = 3.845 A and c = 35.85 A. Capacitance was negative for all frequencies. It was observed that with increase in frequency, value of negative capacitance also increases. It was also observed that real and imaginary dielectric constants, dielectric loss and conductivity were strongly frequency dependent. Negative capacitance also refers to the fact that current lags behind the voltage agitation. Dielectric constant ε' increase with increase in frequency at all temperature ranges but at high frequency it is approximately constant. It exhibit strong dispersion at lower frequencies.

Cavadar *et al.* [33] prepared and investigate the ceramic superconductor. To prepare the sample different materials like $SrCO_3$, $CaCO_3$, Bi_2O_3 and V_2O_5 were mixed in powder form and then heated at 1150 °C for 90 min and then rapidly quenched between copper plates. To identify

the structure and phase purity x-ray diffraction technique was used. Then dielectric charactrisitics i.e real and imaginary parts of dielectric constant, dielectric loss and ac-conductivity were measured over a frequency range of 10KHz to 10MHz at different temperature ranges for 300 K. It was observed that dielectric properties were strongly frequency and temperature dependent. Negative capacitance (NC) phenomenon was also observed. It was concluded that negative capacitance was the result of polarization that occurs at low frequencies causing the deviation of dielectric characteristics. X-ray diffraction of the sample reveals Bi-2212 phase.

Nkum *et al.* [34] investigate the dielectric and transport properties of Indium doped Superconductors. Sample having composition $Bi_{1.84}Pb_{0.34}Sr_{1.91}Ca_{2.03}Cu_{3.06}In_xO_y$ with $0 \leq x \leq 0.15$ was prepared by ordinary solid state method. Basic materials for the preparation of sample were $CaCO_3$, $SrCO3$, Bi_2O_3, PbO and CuO in powdered form. Which were, then mixed and underwent different heat treatments at different temperatures. After that pellets of the samples were prepared and cooled down to room temperature at slow rate at $0.1^{\circ}C$ to $0.2^{\circ}C$ min^{-1}. After preparation of the sample dielectric properties of the sample were measured. Copper wires were connected to both faces of the pellet with silver paste that behaves as conductor in this case. It was noticed in this case that with increase in concentration of Indium, dielectric constant increases as it was the function of polarization. It was stated in the paper that increase in the concentration of Indium may change the basic structure of the sample. It may convert from 2223 phase to 2212 superconducting phase. This may lead to the increase in polarization and as a result increase in dielectric constant. It was also studied in this section that increase in concentration, decreases the dielectric loss. Increase in concentration of the dopant, carrier concentration decreases which may be the result of charge variation and ultimately decreases the holes in the system.

Khan *et al.* [35] studied the dielectric properties of $Cu_{0.5}Tl_{0.5}Ba_2Ca_2Cu_{3-y}Zn_yO_{10-\delta}$ (y = 0, 1.0, 1.5, 2.0, 2.5). They study the changes in dielectric properties by addition of Zn atoms. These properties were studied at room temperature as well as in superconducting state. It was stated in the journal that thermal agitation may increase the polarizability results in enhancement of dielectric constants. They found that $Cu_{0.5}Tl_{0.5}Ba_2Ca_2Cu_{3-y}Zn_yO_{10-\delta}$ in comparison to $Tl_2Ba_2Ca_2Cu_2O_x$ has less dielectric losses and greater conductivity at 290 K and 79 K. They

25

concluded that this low dielectric loss and enhanced conductivity with increased Zn content is due to separation between portable carriers in CuO_2 / ZnO_2 and $Cu_{0.5}Tl_{0.5}Ba_2O_{4-\delta}$ charge reservoir.

Rahim *et al.* [36] studied the effect of temperature and frequency on dielectric characteristics of Cd doped $Cu_{0.5}Tl_{0.5}Ba_2Ca_3(Cy_{4-y}Cd_y)O_{12-\delta}$ (y = 0, 0.25, 0.50, 0.75) superconductors. They prepared the sample by solid state method whereas $Cd(NO_3)_2$, $Ba(NO_3)_2$, $Ca(NO_3)_2$ and $Cu(CN)$ were the basic compounds. Initially all these compounds were in powdered form. They used LCR meter for measurements of capacitance (C) and conductance (G) for frequency ranging from 10 KHz to 10 MHz and temperature ranging from 80 K to 300 K and finally measured the properties like dielectric constant (ε', ε''), dielectric loss (tanδ) and ac conductivity (σ_{ac}). They came to know by increasing the doping of Cd in sample that critical temperature decreases and normal state resistivity increases with increase in Cd concentration. They found out negative capacitance for all $Cu_{0.5}Tl_{0.5}Ba_2Ca_3(Cy_{4-y}Cd_y)O_{12-\delta}$ samples. It was also noticed that higher values of negative capacitance were because of decreased thermal vibrations and greater polarization, at low frequencies and temperatures. This polarization in the sample is because of motion of charges in $CuO2/CdO2$ planes with respect to static charges at Tl^{3+}, Ba^{2+} and Cu^{2+} locations in $Cu_{0.5}Tl_{0.5}Ba_2O_{4-\delta}$ layers by applied external field.

Xiaofeng *et al.* [37] studied Ba based Bi-2222 compounds named layered cuprate $Bi_2Ba_2Nd_{1.6}Ce_{0.4}Cu_2O_{10+\delta}$. They studied dielectric permittivity and also dissipation factor over a range of temperature 80 K to 300 K and frequency ranging from 20 to 10^6 Hz. They found that at low frequency of 1 KHz and room temperature of 300 K dissipation factor was comparatively low and dielectric constant was high (~1000). They argued that polarization is because of hoping of charge carriers between localized sites over potential barriers.

Mumtaz *et al.* [38] investigated the dielectric properties of $Cu_{0.5}Tl_{0.5}Ba_2Ca_2(Cu_{3-y}M_y)O_{10-\delta}$ (M= Si, Ge, Sn, y = 0, 1) superconductor by knowing the values of capacitance (C) and conductance (G) at frequency ranging from 10 KHz to 10 MHz and temperature ranging from superconducting to normal state. They related the greater values of negative dielectrics at low temperatures and frequencies with decreased thermal vibrations because of which polarizability was enhanced. They proposed that smaller values of dielectrics observed in Ge-based

superconductors may be because of high electronegativity of Ge. Sn and Si have almost same value of electronegativity like Cu, therefore, there is no prominent variation in dielectric propertied of 'Sn' and 'Si' based superconductors.

Hashem *et al.* [39] studied dielectric properties of thin films of SnS. These properties were observed at a temperature ranging from 300 to 575 K and frequency ranging from 1 KHz to 100 KHz. Real and imaginary parts of dielectric constant, dielectric loss, ac and dc conductivities of the the sample were studied. It was found that thin films of SnS were the result of thermal evaporation of bulk crystalline SnS. They also found out the activation energy of relaxation and conduction and concluded that it increases or decreases by variation in thickness and frequency.

Chapter 3

SAMPLE SYNTHESIS AND CHARACTERIZATION TECHNIQUES

3.1 Sample Synthesis

A wide range of synthesis techniques have been introduced yet for the synthesis of high temperature superconductors. Purpose of all these techniques is to prepare fine crystalline structure by using synthetic or naturally existing raw material.

Solid state reaction technique is one of the most widely used synthesis techniques for preparation of polycrystalline materials using solid reactants. These reactants are selected depending on conditions of reaction and nature of products. These materials are then mixed in appropriate ratios and grounded using mortar and pestle. During grinding some organic liquid is added to make it homogenous. But it must be evaporated during process of grinding. This material is then put in quartz boat for heat treatment. To increase the contact strength between grains, the material must be pelletized before heat treatment.

Solid-state reaction method has been commonly used for preparation of many cuprates superconductors. To prepare ceramics with all solid materials, metal oxides, nitrates, carbonates and salts are mixed and underwent heat-treatment for a specific period of time till reaction completion [40]. Tl_2O_3 is one of highly toxic material [41]. Therefore, safety measurements must be accounted for preparation of thallium cuprates. Tl-based high T_c superconducting materials were prepared by Sheng and Hermann by heating precursor Ba-Ca-Cu-O with Tl_2O_3 powder for 10 min. at temperature of ~880 – 910°C in flowing oxygen [42-43]. Due to higher volatility of Tl, synthesis of pure phase sample is difficult. In order to prevent greater Tl losses, samples must be wrapped in gold foil. Sealed quartz tubes have also been used for preparation of Tl-based compounds [44-50].

3.1.2 Sample Preparation

$Cu_{0.5}Tl_{0.5}Ba_2Ca_2Cu_3O_{10-\delta}$ samples with different wt. % of carbon nanotubes (CNTs) were prepared by solid-state reaction method in three steps [51]. Starting compounds $Ba(NO_3)_2$, $Ca(NO_3)_2$ and $Cu(CN)$ were mixed in appropriate ratios and ground in mortar and pestle for one hour. After grinding, material was placed in quartz boat for firing in chamber furnace at 860°C. In second step, required wt. % of CNTs were mixed with precursor material and ground well for one hour. Later on the ground material was again fired in quartz boat at 860°C. In third step, Tl_2O_3 was mixed in appropriate ratios in precursor material and the ground material again ground well. Under the pressure of 3.8 tons / cm^3, material was pelletized and then packed in gold capsule for sintering at temperature of 860°C for duration of 10 min followed by quenching at room temperature to obtain $(CNT)x/CuTl$-1223 nano-superconductor composites [52].
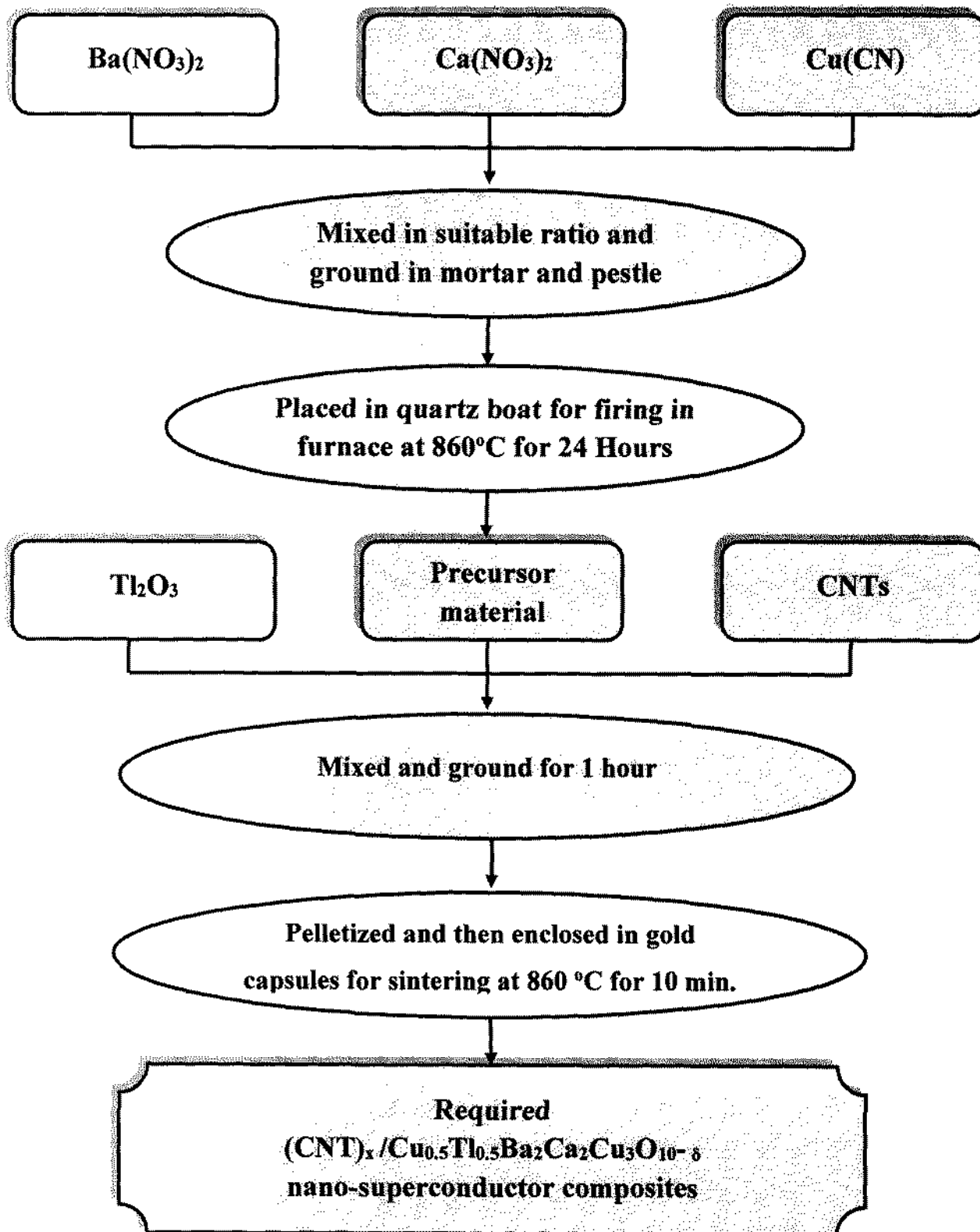
29

Fig. 3.1: Flow chart of synthesis of $(CNT)_x/Cu_{0.5}Tl_{0.5}Ba_2Ca_2Cu_3O_{10-\delta}$ nano-superconductor composite

3.2 Characterization Techniques

Different characterization techniques have been used to investigate various aspects of these nano-superconductor composites. X-Ray diffraction technique is used to find out the internal structure of the nanocomposite crystal [53]. Other techniques like scanning electron microscopy and transmission electron microscopy can also be used to characterize the material. LCR meter is used to find the dielectric properties of material.

3.2.1 X-ray Diffraction (XRD)

X-ray diffraction (XRD) technique is used to determine crystalline phases, grain size, phase composition, defects in structure etc. [54]. X-rays are the electromagnetic radiations of extremely small wavelength ($\sim 10^{-10}$ m). Energy of these radiations is greater than all other electromagnetic radiations which are generated as a result of inner shell transition. Due to extremely small wavelength of XRD, they can penetrate the material [55].

Atoms in crystal diffract X-rays to different angles. By measuring the intensities and angles of diffracted beams, three dimensional image of the density of electron can be constructed. With the help of this electron density, we can find out the position of electron in crystal. As the X-ray beams are diffracted through inter-atomic spacing reflect from the planes of the crystal and interfere according to Brag's Law [56]. i.e.

$$2d\sin\theta = n\lambda \qquad (3.1)$$

Where beams interfere constructively, there we get peak of X-ray diffraction pattern. Diffraction of X-ray from crystal is shown in Fig 3.2.

31
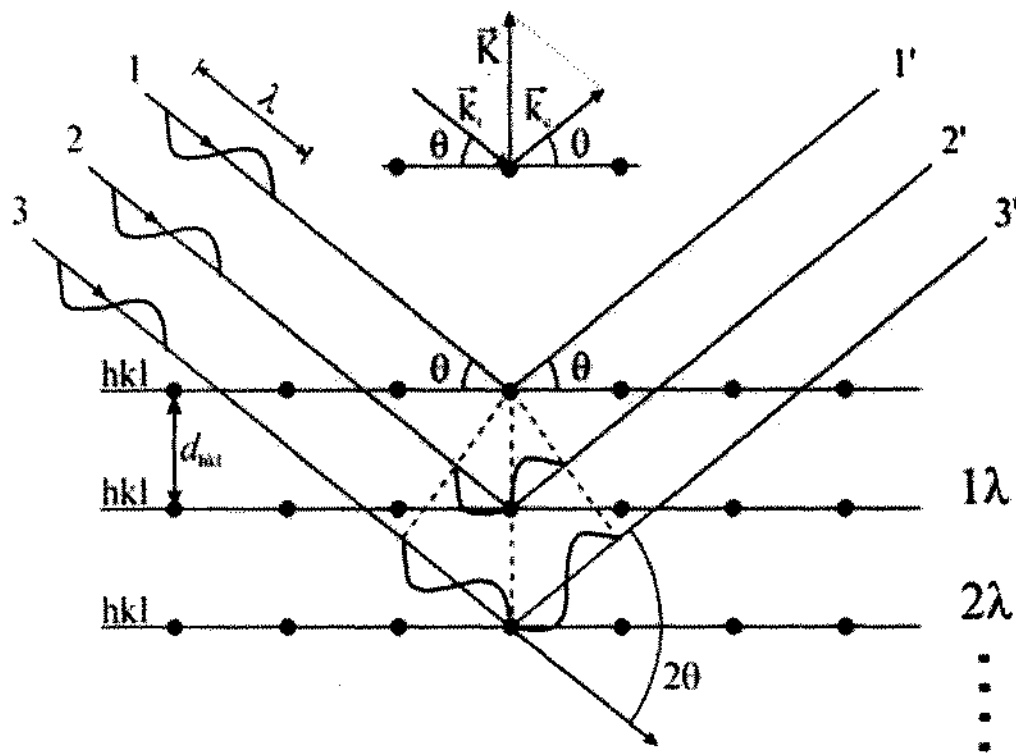
Fig. 3.2: X-ray diffraction

XRD technique may also be used to find the thickness of the thin films and even atomic arrangement is case of glassy solids.

With the help of XRD, measured intensities can provide the exact information about the atomic arrangements in multilayer. XRD is a nondestructive technique and can be used in various atmospheres. In the experimental setup shown in Fig 3.3, 2θ is an angle between incident and diffracted X-rays. Here diffracted intensity is a function of 2θ and orientation of the sample, which produce diffraction pattern. The wavelength of X-ray is ranging from $0.7 - 2$ Å corresponding to energies of $6 - 17$ KeV.
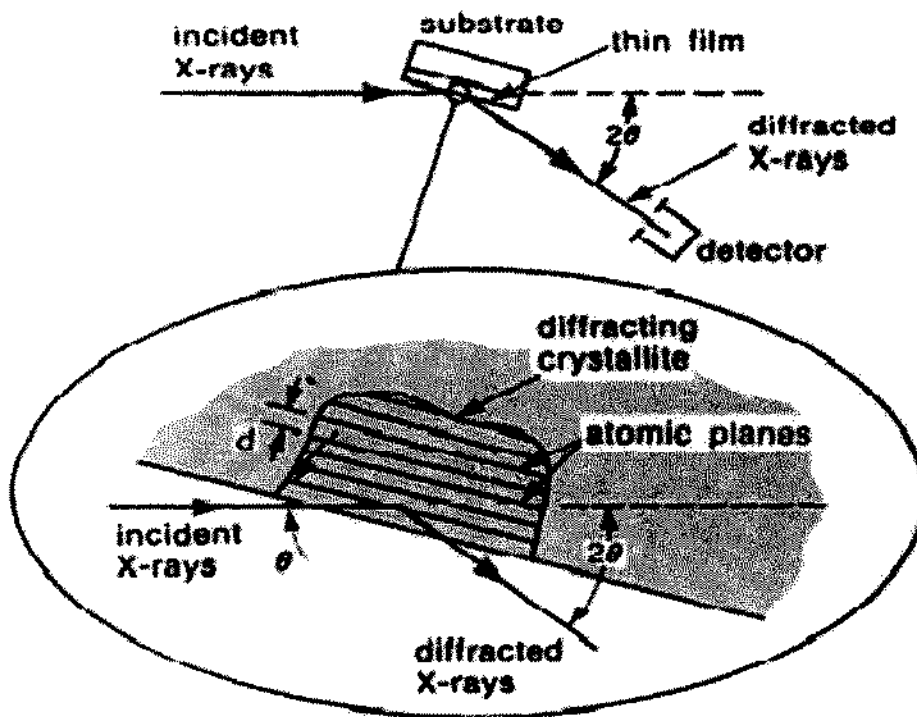
Fig. 3.3: Detailed description of XRD experiment

3.2.2 Scanning Electron Microscope (SEM)

Scanning electron microscope is an advance form of microscope that uses beam of electrons instead of light. Resolution power of SEM is very high, which make it much useful. It has many other advantages over ordinary microscope like broader depth of field because of which greater area of specimen can be examined at once. Degree of magnification can be controlled very easily because in case of SEM electromagnets are used instead of lenses [57].

A typical SEM consists of electron gun, two condensers, objective and detection system. Electron gun is responsible for generation and acceleration of electron beam having energy ranging from 1 KeV to 30 KeV. Three stage lens system demagnified the beam of electron so that it may focus on sample having diameter of 1 nm to 10 nm carrying current 1 pA to 100 pA. If we increase the electron probe diameter upto 0.1 nm to 1 μm, current will be increased from 1nA to 10 nA. Electron beam that comes out from the final lens interact with sample upto depth of 1 μm and ultimately produces signal for the image formation [58].

33
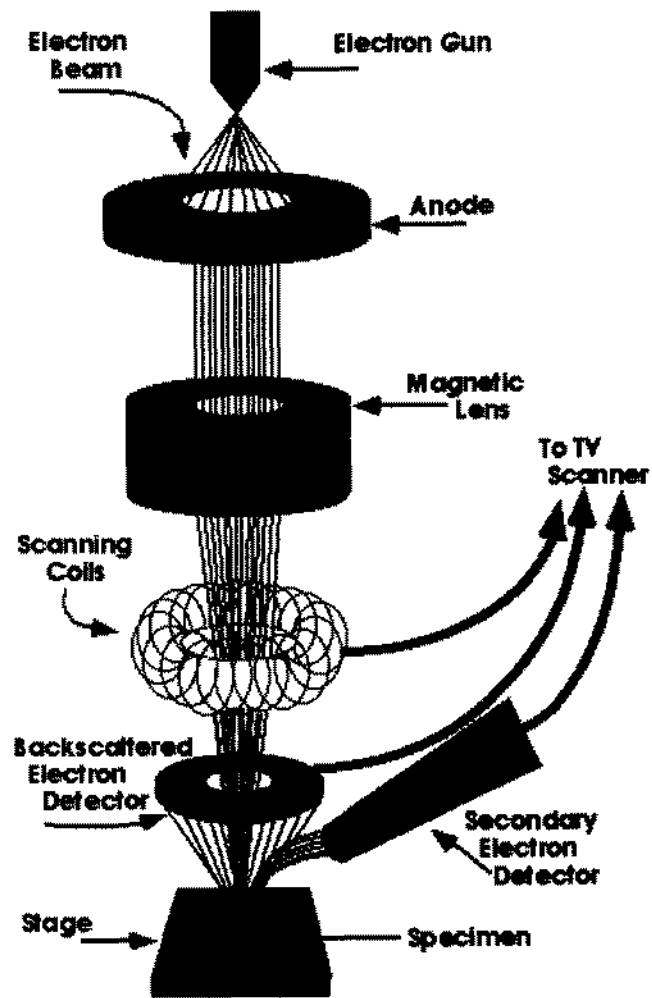
Fig. 3.4: Schematic diagram of scanning electron microscope (SEM)

When electron beam emitted from electron gun interacts with the sample under investigation, it causes the emission of secondary electrons, backscattered electron, auger electrons and photons. Detectors are used to collect these secondary electrons and backscattered electrons, Auger electrons and x rays. Ultimately these detectors convert all of them into signals, which are being used for the generation of final image.

34
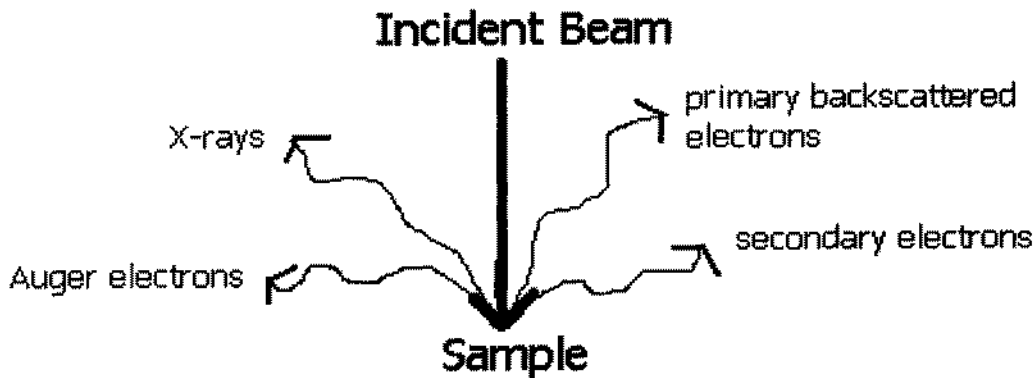
Fig. 3.5: Emission of electrons and photons

3.2.2.1 Secondary Electrons

Beam of electrons that is emitted from electron gun is made incident on the specimen, penetrates into the surface and make inelastic collision with atoms close to the surface of the specimen. In this phenomenon electrons that are close to surface escape from the surface and are named as secondary electrons. These electrons are low energy electrons, having energy less than 50 eV. Most of them exist in the energy range of 0.5 eV to 5 eV [59].

3.2.2.2 Backscattered Electrons

Some of the incident electrons are scattered back from the deeper levels of the specimen. These electrons make elastic collision and after a number of elastic collisions they escape from the specimen. These are known as backscattered electrons. The energy range of this type of electrons is very high i.e. ranging from 50 eV to that of the energy of the incident beam [60].

3.2.2.3 Auger Electrons

Auger electron is the result of Auger Effect. It is actually the alternate to the X-ray emission, which results in de-excitation of the atom to its ground state. When incident electron ejects the electron from 1st shell to any higher, a hole is generated. This may be filled by electron from higher shell resulting in emission of photon of X-ray spectrum. But sometimes this photon

35

is utilized to eject the electron of higher shell. This ejected electron is called Auger Electron as shown in Fig.3.6.
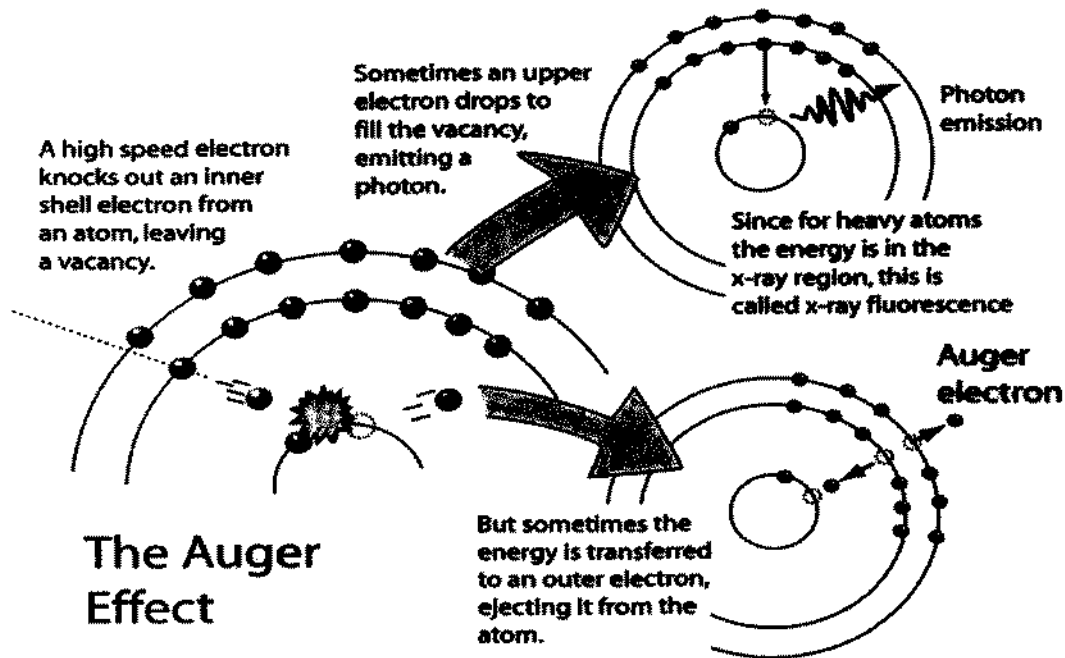
Fig. 3.6: Explanation of Auger Effect.

They escape from the region close to the surface. The auger electrons have energy that depends on the structure of the atom so these electrons provide the chemical composition of sample and so it is a well recognized technique to explain the chemistry of the surface of specimen [61].

3.3 Dielectric Measurements

We have investigated the dielectric properties of the carbon-nanotubes superconductor composites samples, which are given as follow;

1. Dielectric Properties
   a. Real part of Dielectric Constant (ε_r')
   b. Imaginary part of Dielectric Constant (ε_r'')
2. Dielectric loss (tan δ)
3. AC Conductivity (σ_{ac})

3.4　How to prepare sample for Dielectric Measurements?

In order to measure the above said properties, we have to find certain parameters like capacitance and conductance associated with these properties. For this purpose, we connect the sample with LCR meter with help of 4 BNC wires. To prepare the sample first of all we make rectangular geometry of the sample then connect the electrodes with help of silver paste. Silver paste on both sides of the sample behaves as conducting plates and interior of the sample behave like dielectric. In this way a parallel plate capacitor is formed. Then we measured the capacitance and conductance of the sample in the range of frequency 10 KHz to 10,000 KHz at temperature from 77 K to 287 K.

To vary the temperature form 287 K to 77 K, we lower down the sample in container having liquid nitrogen. Temperature was measured by corresponding voltage. At different constant values of temperature, we measured 'C' and 'G' at different frequencies.

We measured following parameters by using given relations [62].

1. Real part of Dielectric Constant

$$\varepsilon_r^{/} = Cd / A\varepsilon_o \tag{3.2}$$

2. Imaginary part of Dielectric Constant

$$\varepsilon_r^{//} = Gd / \omega A\varepsilon_o \tag{3.3}$$

3. Dielectric Loss

$$\tan \delta = \varepsilon_r^{//} / \varepsilon_r^{/} \tag{3.4}$$

4. AC Conductivity

$$\sigma_{ac} = \omega \varepsilon_r^{/} \varepsilon_o \tan \delta \tag{3.5}$$

Where $\omega = 2\pi f$, 'f' is the frequency of 'ac' field in Hz, 'd' is the thickness of the sample, 'C' is capacitance, 'G' is conductivity and 'A' is the area of the plates and '$\varepsilon_o = 8.85 \times 10^{-12}$ F/m' is the permittivity of free space.

3.5 LCR Meter Experimental Setup

To find out the parameters like 'C" and 'G', an HP 4275 A multi frequency LCR meter was used [63]. P-2000/E multimeter was used to measure the voltage drop in reference to temperature. A brass rod having sample holder was used to lower down the sample in cryostat having liquid nitrogen in it. The schematic diagram for dielectric measurements setup is shown in Fig. 3.7.
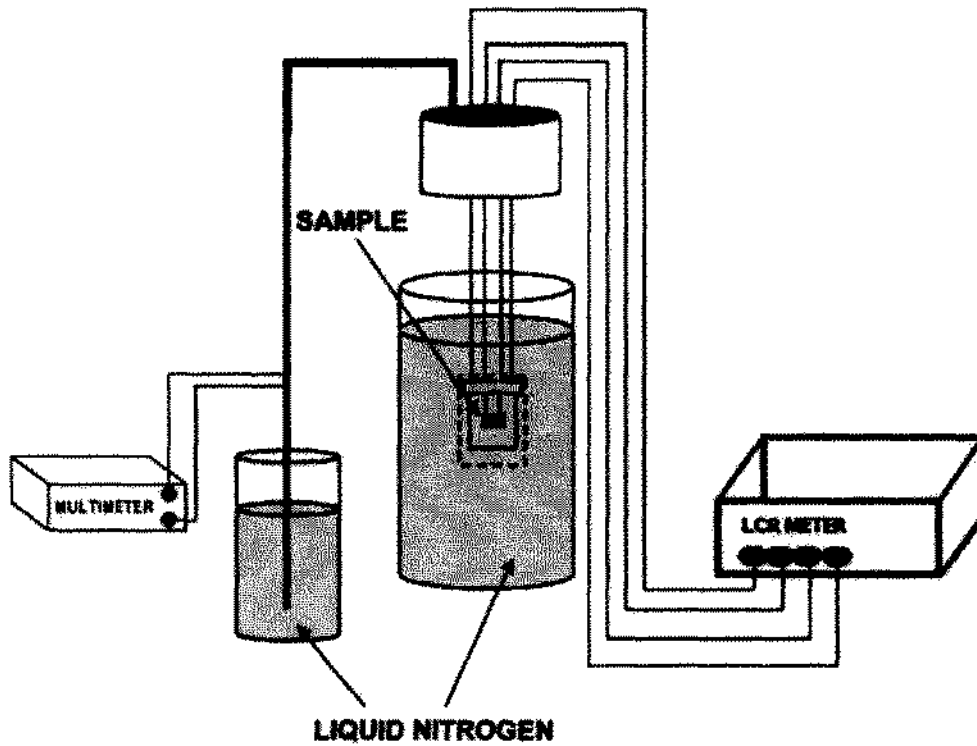

Fig. 3.7: The experimental set-up for the dielectric measurements.

Chapter 4

RESULTS AND DISCUSSION

4.1 X-ray Diffraction

X-ray diffraction (XRD) scans of $(CNTs)_x$/CuTl-1223 with x = 0 and 2.0 wt. % of carbon nanotubes (CNTs) are shown in Fig 4.1. Most of the diffraction peaks are in accordance with orthorhombic crystal structure following PMMM space group. Cell parameters are calculated for the sample by computer software. After addition of CNTs with x=2.0 wt. % cell parameters are a = 4.13Å, b = 4.36 Å, c = 14.17 Å and for sample with x = 0 are a = 4.16 Å, b = 4.46 Å and c = 14.18 Å. Cell parameters before and after addition of CNTs are approximately same as there is no prominent change in cell parameters. So there is not any noticeable change in crystal structure and stoichiometery of the final compound. Addition of CNTs in host CuTl-1223 matrix possibly heal up pores or voids at the grain boundaries. Slight variation in cell parameters after addition of CNTs may be due to stresses and strains produced in the material and oxygen (O_δ) content after addition of CNTs. XRD spectra also confirms the slight shift of variation of peak towards greater angles. This is possibly due to strain produced in material after addition of CNTs. There are also some other very low intensity diffraction peaks observed in XRD spectra which are represented by different symbols. These peaks represent the presence of other superconducting phase (i.e. CuTl-1234) in these composite samples.

4.2 Scanning Electron Microscopy

Scanning electron microscopy (SEM) was used to study the morphology of the $(CNTs)_x$/CuTl-1223 nano-superconductor composite before and after the addition of CNTs. Electron micrograph of CuTl-1223 superconductor with x = 0 and 2.0 wt. % of CNTs is shown in Fig. 4.2 (a, b). It is clear from the micrograph of CuTl-1223 with x = 0, that there are gaps at the inter-grain boundaries. CNTs can be easily visualized in SEM of $(CNTs)_x$/CuTl-1223 with x=2.0 wt. %, which are connecting the grains. After addition of CNTs in CuTl-1223 sample, the activation energy of reaction may help small sized grain to grow and fuse together [64]. These small sized grains not only fuse together but also attached to surface of large size grains. Whereas large sized grain connect each other by multi-walled CNTs. Most likely carbon of these

CNTs is diffused across grain boundaries and responsible for suppression of critical temperature of final compound. CNTs also make electrical connection between grains and provide a path for inter-granular flow of current. These micrographs show that by increasing wt. % of CNTs, surface to volume fraction of final compound is enhanced.
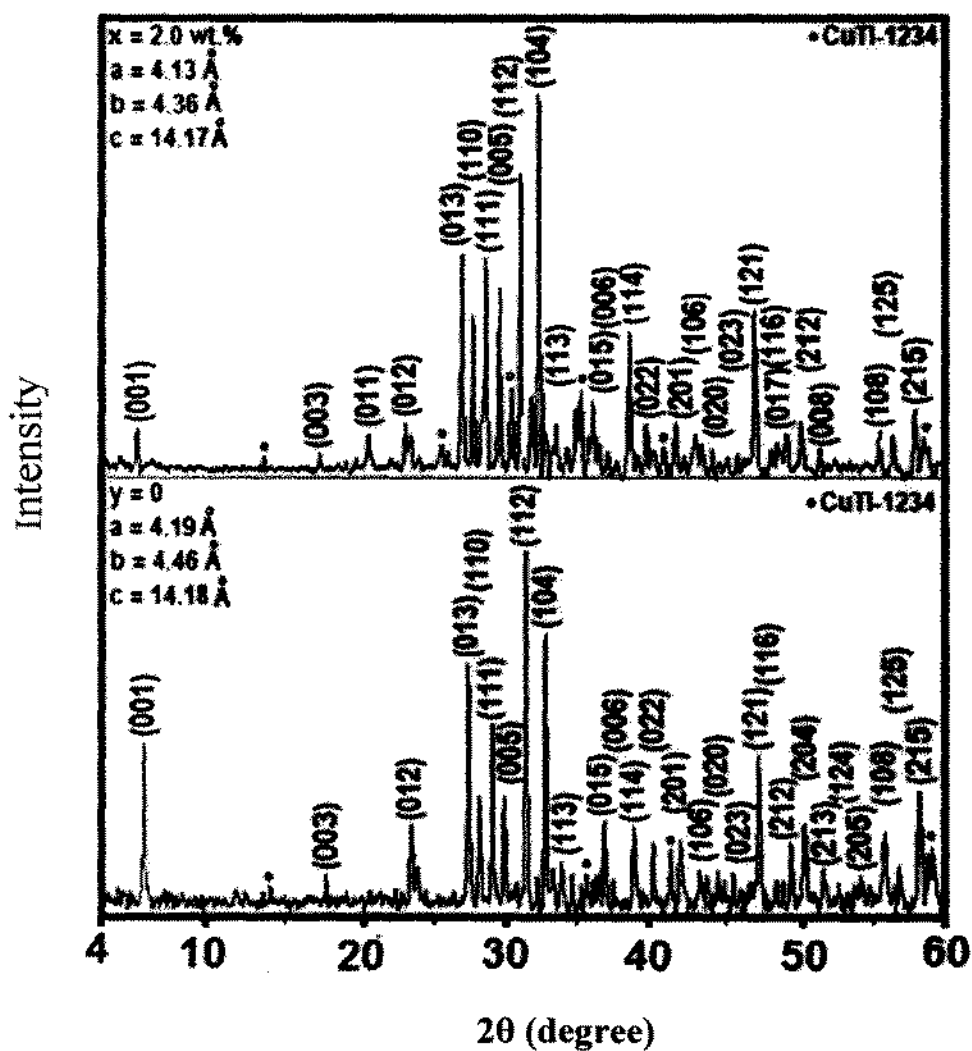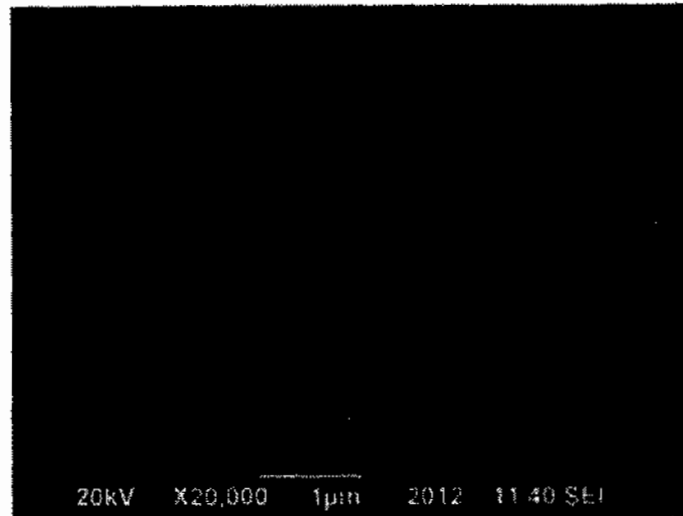

Fig. 4.1: XRD of carbon nanotubes added CuTl-1223 superconductor under x=0 and x=2.0 wt. %

Fig. 4.2: Scanning electron micrograph (SEM) of (CNTs)$_x$/CuTl - 1223 nano-superconductor composites with (a) x = 0, (b) x = 2.0 wt. %.

4.3 Resistivity

The variation of resistivity versus temperature of $(CNTs)_x$/CuTl-1223 nano-superconductor composites with different concentrations of CNTs (i.e. $x = 0$ and 2.0 wt. %) is shown in Fig. 4.3. It is clear from these measurements that variations of resistivity are metallic from room temperature down to onset of superconductivity. Resistivity of un-added pure CuTl-1223 sample is 3.7×10^{-4} Ω-m whereas for CNTs added $(CNTs)_x$/CuTl-1223 sample is 5.3×10^{-4} Ω-m at room temperature. This shows that normal state resistivity increases with addition of CNTs in host CuTl-1223 matrix. This may be due to increased scattering cross section of carriers in sample. Another possible reason may be variation of carrier's density in sample. The zero resistivity critical temperature T_c (0) of $(CNTs)_x$/CuTl-1223 are 90 K and 77 K for $x = 0$ and 2.0 wt. % respectively. The onset of superconductivity transition temperature of $(CNTs)_x$/CuTl-1223 nano-superconducting composites varies from 110 K to 104 K for $x = 0$ and 2.0 wt. % respectively. The suppression of superconducting properties of CuTl-1223 matrix after the inclusion of CNTs can be attributed to semi-conducting nature of these CNTs at superconducting state which reduces the superconducting volume fraction of the final compound.

The reduction of superconducting volume fraction after the inclusion of CNTs may decrease the mobile carriers density, which ultimately suppresses the superconducting properties.
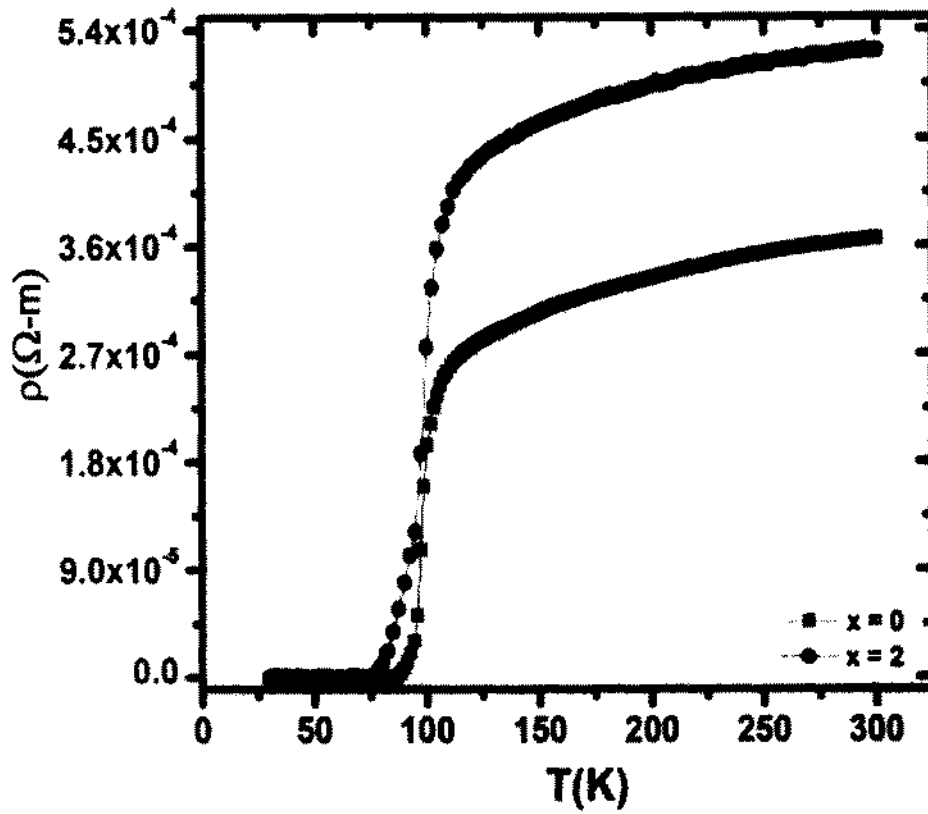
Fig. 4.3: Resistivity versus temperature measurements of $(CNTs)_x/CuTl-1223$ (x = 0, 2.0 wt. %) nano-superconductor composites.

4.4   Dielectric Properties

4.4.1   Real part of Dielectric Constant (ε_r')

This can be calculated by using the relation [65],

$$\varepsilon_r' = Cd \,/\, A\varepsilon_0 \tag{4.1}$$

Where 'C' is the capacitance and 'd' is the thickness.

Real part of dielectric constant (ε_r') determines the value of energy stored within the material when exposed to electric field. The energy may be stored within the grain or at grain-boundaries of the bulk material. Fig 4.4 (a - d) represents the variation in (ε_r') for different values of CNTs (x = 0, 0.25%, 0.5% and 2.0%) in $(CNTs)_x/CuTl$-1223 . Maximum value of ε_r' varies from -494 ~ -427, -558.9 ~ -378.4, -293.6 ~ -29.66, -331.9 ~ -29.66, with concentration of x = 0, 0.25, 0.5 and 2.0 wt. % at temperature ranging from 92 K to 287 K respectively. There is a gradual decrease in ε_r', which may be due to decrease in polarization after CNTs inclusion [66]. At higher frequencies ε_r' is not much affected as there is less polarization at high frequencies. Negative value of ε_r' is because of negative capacitance (NC) [67]. This NC is the decrease in capacitance of sample than its geometric capacitance without sample. This is because of positive space charges within the vicinity of electrodes [68]. The dipolar polarization is result of relative displacement of mobile charges from equilibrium position to that of immobile charges. Flow of free carriers most likely is towards metal electrodes from ceramic sample because of higher Fermi level of ceramics [69-70]. It is believed that this NC phenomenon is the result of electric polarization within the material. There are several other material in which NC has been observed [71 -73]. It is reported in these studies that NC is because of trapping of carriers at metal semiconductor interface, space charge effects and contact injection [67].

4.4.2 Imaginary part of Dielectric Constant (ε_r'')

The imaginary part of dielectric constant (ε_r'') provides the information about dielectric losses of material. It determines dissipation of energy within material under externally applied electric field. In other words it provides the attenuation of energy across interfaces, which involve the grain-boundaries and localized effects. This function is purely frequency dependent and can be calculated by using relation;

$$\varepsilon_r'' = Gd / \omega A\varepsilon_o \tag{4.2}$$

Fig 4.5(a-d) represents the variation in ε_r'' for different values of frequency at temperature ranges from 92 K to 287 K. Imaginary part of dielectric constant increases at lower frequencies and decreasing temperatures for a specific wt. % of CNTs. Maximum attenuation of energy is observed for un-added sample at 92 K and 10 KHz, whereas lowest energy loss is observed at maximum concentration of x = 2.0 wt. % at 92 K and 10 KHz. The value of ε_r'' varies from $1.34 \times 10^9 \sim 7.18 \times 10^8$, $9.06 \times 10^8 \sim 7.61 \times 10^8$, $2.8 \times 10^8 \sim 1.28 \times 10^8$ and $1.78 \times 10^6 \sim 7.2 \times 10^5$ for concentration of CNTs (x = 0, 0.25, 0.5 and 2.0 wt. %) at 10 KHz. It shows that energy loss decreases with increase in wt. % of CNTs in composite materials, which can be attributed to the semiconducting nature of CNTs. The presence of these CNTs at grain-boundaries reduces the polarization and facilitates the carriers to move in the bulk material. The carrier's accumulation at the interfaces (grain-boundaries) has been reduced, which reduces the main polarization (interfacial polarization) contributing to the dielectric parameters.
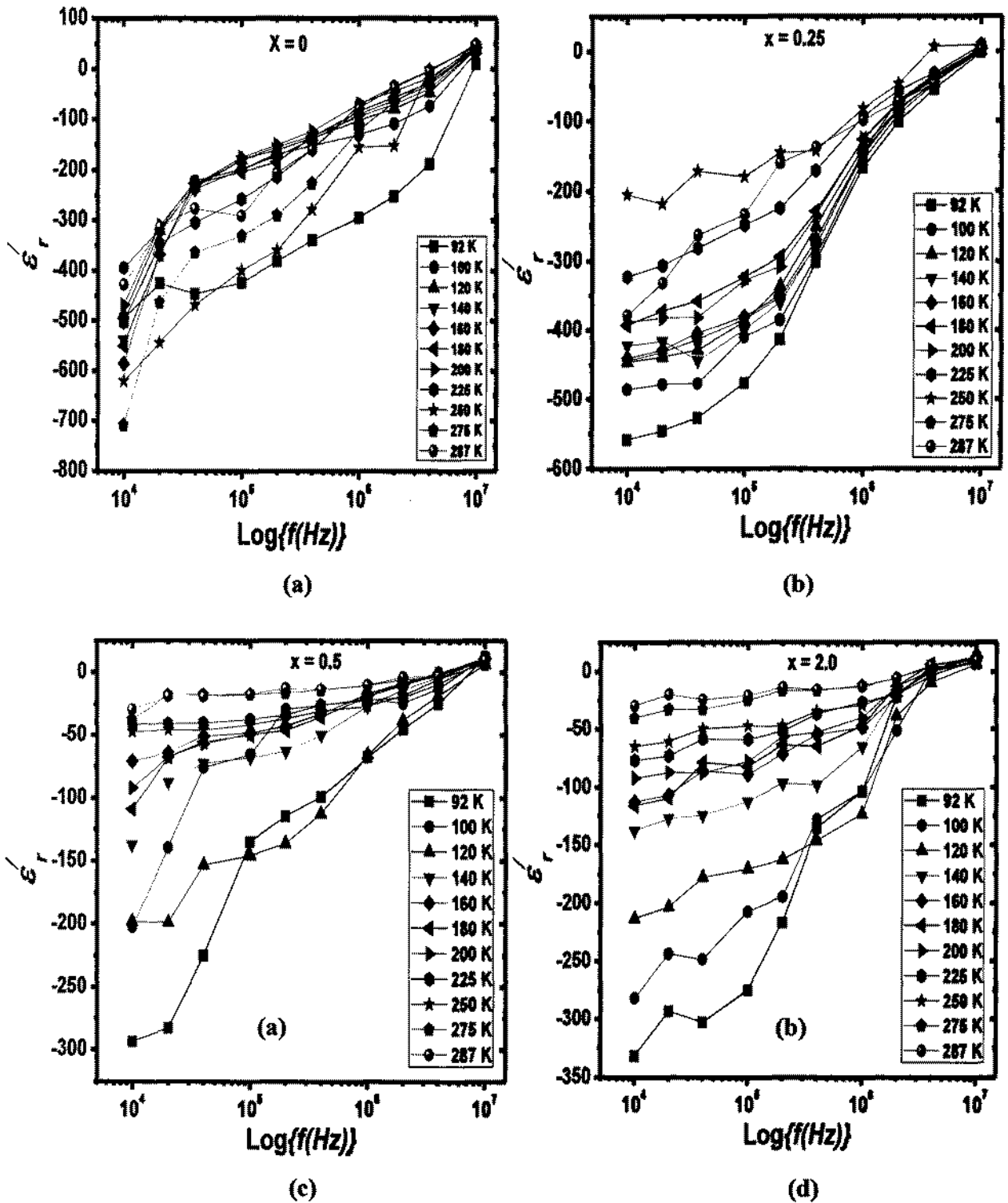
Fig. 4.4: Real part of dielectric constant (ε_r') versus Log{f(Hz)} of CuTl-1223 composite for (a) x = 0, (b) x = 0.25 wt. %, (c) x = 0.5 wt. %, (d) x = 2.0 wt. %.

Fig. 4.5: Imaginary part of dielectric constant (ε_r'') versus Log{f(Hz)} of CuTl-1223 composite for (a) x = 0, (b) x = 0.25 wt. %, (c) x = 0.5 wt. %, (d) x = 2.0 wt. %.

4.4.3 AC Conductivity (σ_{ac})

The ac-conductivity of $(CNTs)_x$/CuTl-1223 nano-superconductor composites as a function of frequency at different operating temperatures is shown in Fig 4.6 (a - d). For un-added pure CuTl-1223 sample, ac- conductivity is maximum at lower frequency of 10 KHz at 92 K. Value of σ_{ac} versus Log{f(Hz)}varies from 0.328 ~ 0.173, 0.221 ~ 0.209, 0.062 ~ 0.035, 0.022 ~ 0.012 at concentration of x = 0, 0.25, 0.5 and 2.0 wt. % respectively, at different frequencies and operating temperature ranging from 92 K to 287 K. It is clear from Fig 4.6 that σ_{ac} of these composite materials decreases with increasing wt. % of CNTs. At high frequencies, σ_{ac} is almost zero for all samples at temperature range of 92 K to 287 K but at low frequencies it strongly depends on operating temperature. The gradual increase in σ_{ac} with decreasing operating temperature shows lower scattering cross-section of mobile carriers nearer to critical temperature [74]. After addition of CNTs in CuTl-1223 matrix, value of σ_{ac} decreases, which may likely be due to decreased carrier's density in $(CNTs)_x$/CuTl-1223 nano-superconductor samples [75]. Decrease in σ_{ac} may also be due to semiconducting nature of CNTs, which reduces carrier's mobility through grain-boundaries at lower operating temperatures, resulting in decreased values of σ_{ac}.

Fig. 4.6: ac - conductivity (σ_{ac}) versus Log{f(Hz)} of CuTl-1223 composite for (a) x = 0, (b) x = 0.25 wt. %, (c) x = 0.5 wt. %, (d) x = 2.0 wt. %.

Conclusion

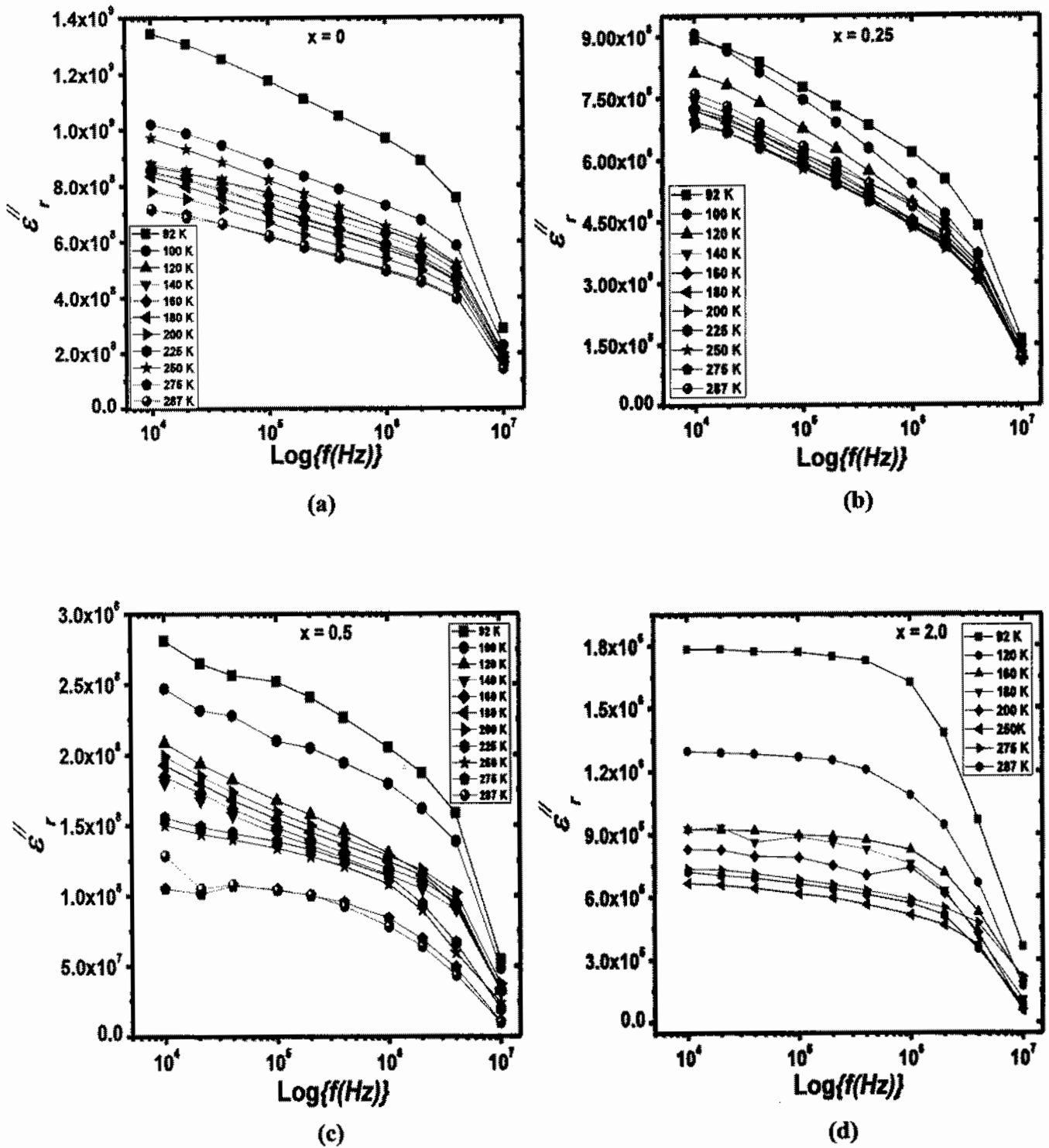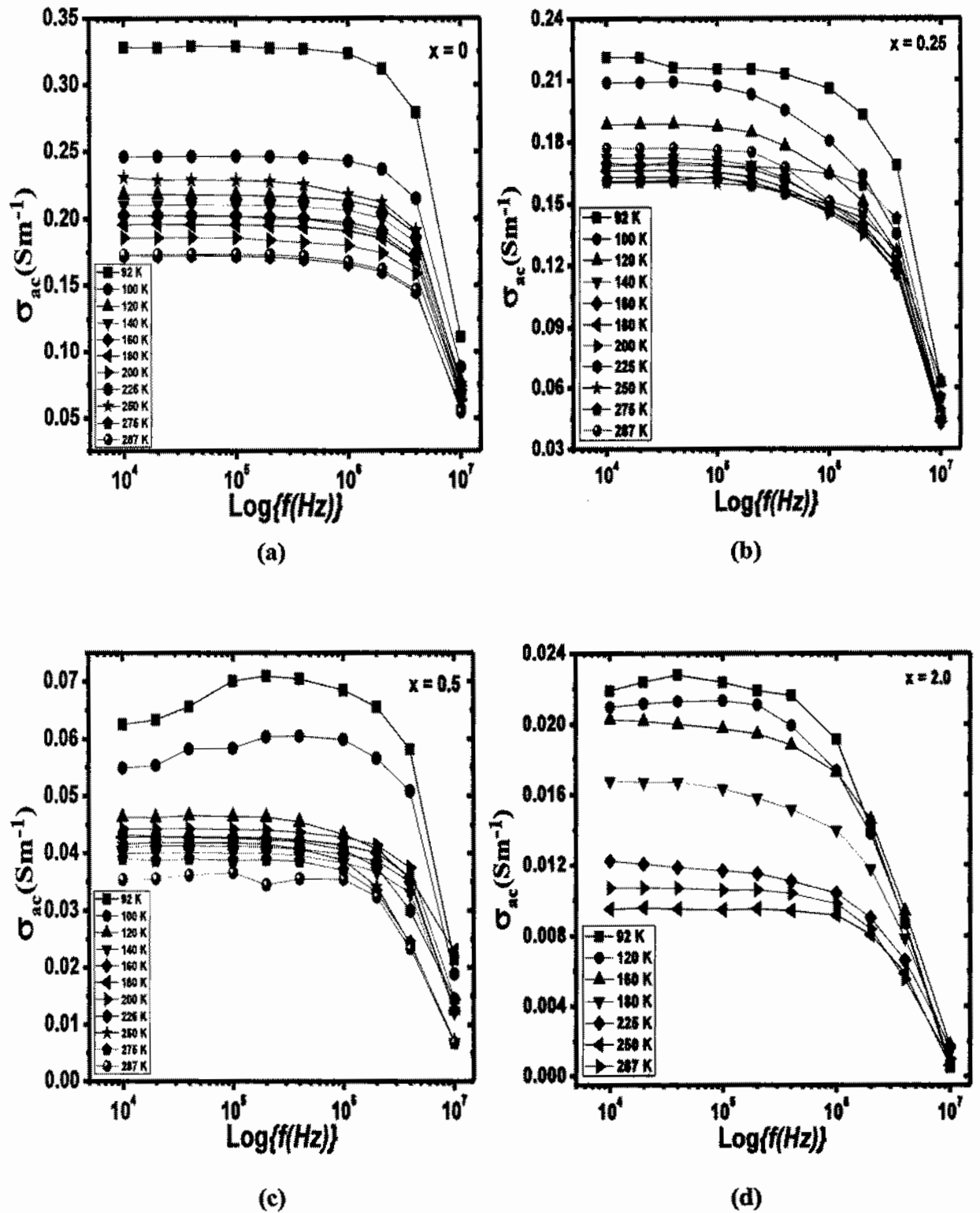(CNTs)$_x$/CuTl-1223 nano-superconductor composites were prepared by solid-state reaction method and characterized by XRD, SEM and dc-resistivity. It was observed that crystal structure was not affected by the addition of CNTs. Morphology of (CNTs)$_x$/CuTl-1223 composite samples was examined by SEM, which showed the improvement of inter-grain weak-links after CNTs addition in CuTl-1223 matrix. Small sized grains fuse together by using the activation energy of reaction. Addition of CNTs in CuTl-1223 decreases the transition temperature with increasing wt. % of CNTs, which is most likely due to reduced superconducting volume fraction and carriers density. Dielectric properties of samples were studied by capacitance (C) and conductance (G) measurements as function of frequency and temperature. Real part of dielectric constant decreases by increasing wt. % of CNTs, which most likely be due to semiconducting nature of CNTs. Addition of CNTs from x = 0 to 2 wt. % also decreases the ac-conductivity (σ_{ac}) of CNTs/CuTl-1223 nano-superconductor composites, which may be due to decreased carrier's density. Imaginary part of dielectric constant ($\varepsilon_r^{//}$) strongly depends upon frequency and temperature and decreases with increase in wt. % of CNTs.

References:

[1]   P. Muller, A.V. Ustinov and V.V. Schmidt, *The Physics of Superconductors*, Springer Science & Business Media (1997).

[2]   M. Cyrot, *Introduction to Superconductivity and High-Tc Materials*, World Scientific (1992).

[3]   Thomas P. Sheahen, *Introduction to High Temperature Superconductivity*, Springer Science & Business Media (1994).

[4]   Mehta Neeraj, *Applied Physics for Engineers*, PHI Learning Pvt. Ltd. (2011).

[5]   Harald Ibach, Hans Lüth, *Solid State Physics: An Introduction to Principles of Materials Science*, 2nd Edition, Springer (1995).

[6]   J.P. Srivastava, *Elements of Solid State Physics*, PHI Learning Pvt. Ltd. (2011).

[7]   Sven Larsson, *Chemical Physics: Electrons and Excitations*, CRC Press (2012).

[8]   S.O Pillai, *Applied Physics*, New Age International (2006).

[9]   I. A. Parinov, *Microstructure and Properties of High-Temperature Superconductors*, 2nd Edition, Springer Science & Business Media (2013).

[10]   Soltan Soltan, *Interaction of Superconductivity and Ferromagnetism in YBCO-LCMO Heterostructures*, Cuvillier Verlag (2005)

[11]   G. Aruldhas, P. Rajagopal, *Modern Physics*, PHI Learning Pvt. Ltd. (2005).

[12]   Rudolf P. Huebener, *Conductors, Semiconductors, Superconductors: An Introduction to Solid State Physics*, Springer (2014)

[13]   Eoin O'Reilly, *Quantum Theory of Solids*, CRC Press (2003).

[14]   Xiao-Feng Pang, Yuan-Ping Feng, *Quantum Mechanics in Nonlinear Systems*, World Scientific (2005).

[15]   Neeraj Mehta, *Textbook of Engineering Physics*, Volume II, PHI Learning Pvt. Ltd. (2009).

[16]   Joshi, *Engineering Physics*, McGraw-Hill Education (2010).

[17]   S.L. Kakani, *Material Science*, New Age International (2006).

[18]   M. S. Vijaya, G. Rangarajan, *Material science*, McGraw-Hill (2003).

[19]   G. Aruldhas , *Engineering Physics* (2010).

[20]   C.P.Smyth, *Annual Review of Physical Chemistry*, **17**, 433(1966).

[21] William D. Callister, David G. Rethwisch, *Fundamentals of Materials Science and Engineering: An Integrated Approach*, John Wiley & Sons (2012)

[22] Preeti Maheshwari, *Electronic Components and Processes*, New Age International (2006).

[23] Gisha. S. George, *Engineering Physics*, Technical Publications (2007).

[24] J. A. Brydson, *Plastics Materials*, 6th edition, Elsevier (1995).

[25] David Richerson, David W. Richerson, William Edward Lee, *Modern Ceramic Engineering: Properties, Processing, and Use in Design*, 3rd Edition, CRC Press, (2006).

[26] John F. Mongillo, *Nanotechnology 101*, ABC-CLIO (2007).

[27] Manasi Karkare, *Nanotechnology: Fundamentals and Applications*, I. K. International Pvt Ltd (2008).

[28] Mikell P. Groover, *Fundamentals of Modern Manufacturing: Materials, Processes, and Systems, 4th edition*, John Wiley & Sons (2010).

[29] Vincent M. Rotello, *Nanoparticles: Building Blocks for Nanotechnology*, Springer Science & Business Media (2004).

[30] Hermann A. M. and Yakhmi J. V., Thallium based high temperature superconductors (1994).

[31] T. S. Kayed, Mater *Res. Bull* **38** 533-538 (2003).

[32] S. Cavdar, H. Koralay, N. Tugluoglu and A. Gunen, *Supercond. Sci. Technol.* **18**, 1204-1209 (2005).

[33] S. Cavdar, H. Koralay, S. Altindal, *J. Low Tem. Phys.* **164**, 102-114 (2011).

[34] R.K. Nkum, M.O. Gyekye, F.Boakye *Solid state Communications* **122**, 569 – 573(2002).

[35] Nawazish A. Khan, M. Mumtaz, A. A. Khurram; *Journal of Applied Physics* **104**, 033916 (2008).

[36] M. Rahim, Nawazish A. Khan, M. Mumtaz, *Journal Low Temperature Physics* **172**:47 – 58 (2013)

[37] Xiaofeng Xu, Zhengkuan jiao, Minyi Fu, Lixin Feng, Kaixun Xu, Rongqing Zuo, Xuezhi. Chen, *Physica C* **417**, 166 – 170, (2005).

[38] M. Mumtaz, Nawazish A. Khan, Sajid Khan; *Journal of Applied Physics* **111**, 013920 (2012).

[39] H. A. Hashem, S. Abouelhassan, Chinese, *Journal of Physics*, Vol **43**,955-966, (2005).

[40] C. N. R. Rae and J. Gopalakrishnan, *New directions in Solid State Chemistry*, Cambridge University Press, Cambridge (1998).

[41] Jeffrey W. Lynn, *High Temperature Superconductivity*, Springer Science & Business Media (2012).

[42] Z.Z. Sheng and A. M. Hermann, Nature **332**, 55 (1988).

[43] Z. Z. Sheng and A. M. Hermann, Nature **332**, 138 (1988).

[44] S.S.P. Parkin, V.Y. Lee, E.M. Engler, A.I. Nazzal, T.C. Huang, G. Gorman, R. Savoy and R. Beyers, Phys. Rev. Lett. **60**, 2539 (1988).

[45] R. Beyers, S.S.P. Parkin, V.Y. Lee, A.I. Nazzal, R. Savoy, G. Gorman, T.C. Huang and S. LaPlaca, Appl. Phys. Lett. **53**, 432 (1988).

[46] S.S.P.Parkin, V.Y. Lee, A. Nazzal, R. Savoy, T.C. Huang, G. Gorman and R. Beyers, Phys. Rev. B **38**, 6531 (1988).

[47] S.S.P. Parkin, V.Y. Lee, A.I. Nazzal, R. Savoy and R. Beyers and S. J. LaPlaca, Phys. Rev. Lett **61**, 750 (1988).

[48] M. Hervieu, C. Michel, A. Maignan, C. Martin and B. Raveau, I. Solid State Chem. **74**, 428 (1988).

[49] M. Hervieu, C. Martin, J. Provost and B. Raveau, J. Solid State Chem. **76**, 419 (1988).

[50] M. Hervieu, A. Maignan, C. Martin, C. Michel, J. Provost and B. Raveau, J. Solid State Chem, **75**, 212 (1988).

[51] Anthony R. West, *Solid State Chemistry and Its Applications*, John Wiley & Sons (1987).

[52] Nawazish A. Khan, Sadaf Aziz, *Journal of Alloys and Compounds* **538**, 183–188 (2012).

[53] Yoshio Waseda, Eiichiro Matsubara, Kozo Shinoda, *X-Ray Diffraction Crystallography*, Springer Science & Business Media (2011).

[54] B. D Cullity, *Elements of x-ray diffraction*, 2nd edition, Addison-wesley publishing company, Inc. London (1977).

[55] C. Suryanarayana, M. Grant Norton , *X-Ray Diffraction: A Practical Approac*, Springer Science & Business Media (1998).

[56] Gregory S. Rohrer, *Structure and Bonding in Crystalline Materials*, Cambridge University Press (2001).

[57] purdue.edu/rem/rs/sem.htm

[58] Anjam Khursheed, *Scanning Electron microscope optics and spectrometers.*

[59] Maurizio Dapor, Springer Science+Business Media, *Transport of Energetic Electrons in Solids: Computer Simulation with Applications to Materials Analysis and Characterization*, Springer (2014).

[60] Ludwig Reimer, *Scanning Electron Microscopy: Physics of Image Formation and Microanalysis*, Springer Science & Business Media (1998).

[61] David Bernard Williams, C. Barry Carter, *Transmission Electron Microscopy: A Textbook for Materials Science*, Volume 1, Springer Science & Business Media (1996).

[62] I. D Doss, John Wiley and sons, *Engineers Guide to High Temperature Superconductivity* , New York (1990).

[63] U.A.Bakshi, A.V.Bakshi, *Electronic Measurement Systems*, Technical Publications (2009).

[64] Nawazish A. Khan, Sadaf Aziz, *Journal of Alloys and Compounds* **538**, 183–188 (2012).

[65] I.M. Afandiyeva, I. Dökme, Altlndal, M.M. Bülbül, and A. Tatarolu: *Microelectron. Eng.* **85**, 247 (2008).

[66] Hana Naceur*, Adel Megriche and Mohamed El Maaoui, *Oriental Journal Of Chemistry*, **29**, (937-944), 2013.

[67] M. Mumtaz, Nawazish A. Khan, Sajid Khan, *IEEE Transactions on Applied Superconductivity*, Vol. **23**, No. 2 (2013).

[68] Adnan Younis and Nawazish Ali Khan, *Journal of the Korean Physical Society*, Vol. **57**, 1437-1443 (2010).

[69] N. A. Khan, M. Mumtaz and A. A. Khurram, *J. Appl.Phys.* **104**, 033916 (2008).

[70] H. G. C, Etinkaya • Sahar Alialy • S , . Altındal • A. Kaya • I ˙. Uslu, *J Mater Sci: Mater Electron* DOI 10.1007/s10854-015-2816-7.

[71] M. Ershov, H. C. Liu, L. Li, M. Buchanan, Z. R. Wasileweki, and V. Ryzhii, *Appl. Phys. Lett.*, **70**, 1828-1830, (1997).

[72] N. C. Chen, P. Y. Wang and J. F. Chen, *Appl. Phys. Lett.*, **72**, 1081-1083, (1998).

[73] A. G. U. Perera, W. Z. Shen, M. Ershov, H. C. Liu, M. Buchanan, W. J. Schaff, *Appl. Phys. Lett.*, **74**, 3167-3169, (1999).

[74] M. Rahim · Nawazish A. Khan · M. Mumtaz; J Low Temp Phys **172**, 47–58 (2013).

[75] N.A. Khan, M. Rahim, J. Alloys Compd. **481**, 81 (2009).